REVIEW ARTICLE

Optical frequency synthesis based on mode-locked lasers

Steven T. Cundiff,[a] Jun Ye, and John L. Hall
JILA, National Institute of Standards and Technology and University of Colorado, Boulder, Colorado 80309-0440

(Received 5 February 2001; accepted for publication 15 July 2001)

The synthesis of optical frequencies from the primary cesium microwave standard has traditionally been a difficult problem due to the large disparity in frequency. Recently this field has been dramatically advanced by the introduction and use of mode-locked lasers. This application of mode-locked lasers has been particularly aided by the ability to generate mode-locked spectra that span an octave. This review article describes how mode-locked lasers are used for optical frequency synthesis and gives recent results obtained using them. © *2001 American Institute of Physics.* [DOI: 10.1063/1.1400144]

I. INTRODUCTION

At the present, measurement of frequencies into the microwave regime (tens of gigahertz) is straightforward due to the availability of high frequency counters and synthesizers. Historically, this has not always been the case, with direct measurement being restricted to low frequencies. The current capability arose because an array of techniques was developed to make measurement of higher frequencies possible.[1] These techniques typically rely on heterodyning to produce an easily measured frequency difference (zero beating being the limit). The difficulty lay in producing an accurately known frequency to beat an unknown frequency against.

Measurement of optical frequencies (hundreds of terahertz) has been in a similar primitive state until recently, despite the enormous effort of many groups around the world to solve this difficult problem. This is because only few ''known'' frequencies have been available and it has been difficult to bridge the gap between a known frequency and an arbitrary unknown frequency if the gap exceeds tens of gigahertz (about 0.01% of the optical frequency). Furthermore, establishing known optical frequencies was itself difficult because an absolute measurement of frequency must be based on the time unit ''second,'' which is defined in terms of the microwave frequency of a hyperfine transition of the cesium atom. This requires complex ''clockwork'' to connect optical frequencies to those in the microwave region.

Optical frequencies have been used in measurement science since shortly after the invention of lasers. Comparison of a laser's frequency of $\sim 5\times 10^{14}$ Hz with its ideal $\sim$ millihertz linewidth, produced by the fundamental phase diffusion of spontaneous emission, reveals a potential dynamic range of 10^{17} in resolution, offering one of the best tools with which to discover new physics in ''the next decimal place.'' Nearly 40 years of vigorous research in the many diverse aspects of this field by a worldwide community have resulted in exciting discoveries in fundamental science and development of enabling technologies. Some of the ambitious long-term goals in optical frequency metrology are just coming to fruition due to a number of recent spectacular technological advances, most notably, the use of modelocked lasers for optical frequency synthesis. Other examples include laser frequency stabilization to 1 Hz and below,[2] optical transitions observed at a few Hz linewidth (corresponding to a Q of 1.5×10^{14}),[3] and steadily improving accuracy of optical standards with a potential target of 10^{-18} for cold atom/ion systems. Indeed, it now seems to be quite feasible to realize, with a reasonable degree of simplicity and robustness, an optically based atomic clock and an optical frequency synthesizer. Considering that most modern measurement experiments use frequency-based metrology, one can foresee tremendous growth in these research fields.

The ability to generate wide-bandwidth optical frequency combs has recently provided a truly revolutionary advance in the progress of this field. In this review we describe the implementation of a frequency measurement technique utilizing a series of regularly spaced frequencies that form a ''comb'' spanning the optical spectrum. The optical frequency comb is generated by a mode-locked laser. The comb spacing is such that any optical frequency can be easily measured by heterodyning it with a nearby comb line. Furthermore, it is possible to directly reference the comb spacing and position to the microwave cesium time standard, thereby determining the absolute optical frequencies of all of the comb lines. This recent advance in optical frequency measurement technology has facilitated the realization of the ultimate goal of a practical optical frequency synthesizer: it forms a phase-coherent network linking the entire optical spectrum to the microwave standard.

The purpose of this review article is to present the recent advances in optical frequency synthesis and metrology that have been engendered by using femtosecond mode-locked lasers to span vast frequency intervals. This surprising union of two apparently disparate realms likely means that few

[a]Electronic mail: cundiffs@jila.colorado.edu

readers will be familiar with both. Therefore, in the following we attempt to address either the optical metrologist wishing to become knowledgeable about ultrafast science or, vice versa, an enabling, albeit challenging, undertaking. In Sec. II we provide background on optical frequency metrology, reviewing the state of the art (prior to the introduction of mode-locked lasers) and the motivation. To put the recent advances into context and to provide comparison, other techniques, which do not employ mode-locked lasers, are reviewed in Sec. III. In sec. IV the basics of mode-locked lasers are covered with emphasis on the characteristics that are relevant to optical frequency synthesis. In Sec. V we describe how the output comb can be controlled in such a way that is suitable for optical frequency synthesis. This is followed by a description of several recent experiments that have demonstrated the dramatic breakthrough that these techniques have enabled. In Sec. VI we discuss the impact of this work on other fields and expected future developments.

II. BACKGROUND: OPTICAL FREQUENCY SYNTHESIS AND METROLOGY

Optical frequency metrology broadly contributes to and profits from many areas in science and technology. At the core of this subject is the controlled and stable generation of coherent optical waves, i.e., optical frequency synthesis. This permits high precision and high resolution measurement of many physical quantities.

In Secs. II A–II C, we will present brief discussions on these aspects of optical frequency metrology, with stable lasers and wide bandwidth optical frequency combs making up the two essential components in stable frequency generation and measurement.

A. Establishment of standards

In 1967, just a few years after the invention of the laser, the international standard of time/frequency was established, based on the $F=4$, $m_F=0 \rightarrow F=3$, $m_F=0$ transition in the hyperfine structure of the ground state of ^{133}Cs.[4] The transition frequency is defined to be 9192 631 770 Hz. The resonance Q of $\sim 10^8$ is set by the limited coherent interaction time between matter and field. Much effort has been invested in extending the coherent atom–field interaction time and in controlling the first and second order Doppler shifts. Recent advances in laser cooling and trapping technology have led to the practical use of laser-slowed atoms, and a 100-fold resolution enhancement. With the reduced velocities, Doppler effects have also been greatly reduced. Cs clocks based on atomic fountains are now operational, with reported accuracy of 3×10^{-15} and short-term stability of 1×10^{-13} at 1 s, limited by the frequency noise of the local rf crystal oscillator.[5] Through similar technologies, single ions, laser cooled and trapped in an electromagnetic field, are now also excellent candidates for radio frequency/microwave standards, with a demonstrated frequency stability approaching 3×10^{-13} at 1 s.[6] More compact, less expensive (and less accurate) atomic clocks use cesium or rubidium atoms in a glass cell equipped with all essential clock mechanisms, including optical pumping (atom preparation), microwave circuitry for exciting the clock transition, and optical detection. The atomic hydrogen maser is another mature and practical device that uses the radiation emitted by atoms directly.[7] Although it is less accurate than the cesium standard, a hydrogen maser can realize exceptional short-term stability.

The development of optical frequency standards has been an extremely active field since the invention of lasers, which provide the coherent radiation necessary for precision spectroscopy. The coherent interaction time, the determining factor of the spectral resolution in many cases, is in fact comparable in both optical and rf domains. The optical part of the electromagnetic spectrum provides higher operating frequencies. Therefore the quality factor, Q, of an optical clock transition is expected to be a few orders higher than that available in the microwave domain. A superior Q factor helps to improve all three essential characteristics of a frequency standard, namely, accuracy, reproducibility, and stability. Accuracy refers to the objective property of a standard to identify the frequency of a natural quantum transition, idealized to the case that the atoms or the molecules are at rest and free of any perturbation. Reproducibility measures the repeatability of a frequency standard for different realizations, signifying adequate modeling of observed operating parameters and independence from uncontrolled operating conditions. Stability indicates the degree to which the frequency stays constant after operation has started. Ideally, a stabilized laser can achieve a fractional frequency stability

$$\frac{\delta v}{v} = \frac{1}{Q}\frac{1}{\mathrm{S/N}}\frac{1}{\sqrt{\tau}},$$

where S/N is the recovered signal-to-noise ratio of the resonance information, and τ is the averaging time. Clearly it is desirable to enhance both the resolution and sensitivity of the detected resonance, since they control the time scale necessary for a given measurement precision. The reward is enormous: enhancing the Q (or S/N) by a factor of 10 reduces the averaging time by a factor of 100.

The nonlinear nature of a quantum absorption process, while limiting the attainable S/N, permits sub-Doppler resolution. Special optical techniques invented in the 70s and 80s for sub-Doppler resolution include saturated absorption spectroscopy, two-photon spectroscopy, optical Ramsey fringes, optical double resonance, quantum beats, and laser cooling and trapping. Cold samples offer a true possibility to observe the rest frame atomic frequency. Sensitive detection techniques, such as polarization spectroscopy, electron shelving (quantum jump), and frequency modulation optical heterodyne spectroscopy, were also invented during the same period, leading to an absorption sensitivity of 1×10^{-8} and the ability to split a MHz scale linewidth typically by a factor of 10^4–10^5 at an averaging time of $\sim$1 s. All these technological advances paved the way for subhertz stabilization of supercoherent optical local oscillators.

To effectively use a laser as a stable and accurate optical local oscillator, active frequency control is needed due to the strong coupling between the laser frequency and the laser parameters. The simultaneous use of quantum absorbers and an optical cavity offers an attractive laser stabilization system. A passive reference cavity brings the benefit of a linear

response, allowing the use of sufficient power to achieve a high S/N. On one hand, a laser pre-stabilized by a cavity offers a long phase coherence time, reducing the need for frequent interrogations of the quantum absorber. In other words, the laser linewidth over a short time scale is narrower than the chosen atomic transition width and thus the information of the natural resonance can be recovered with an optimal S/N and the long averaging time translates into a finer examination of the true line center. On the other hand, the quantum absorber's resonance basically eliminates inevitable drifts associated with material standards, such as a cavity. Frequency stability in the 10^{-16} domain has been measured with a cavity-stabilized laser.[8] The use of frequency modulation for cavity/laser lock has become a standard laboratory practice.[9] Tunability of such a cavity/laser system can be obtained by techniques such as the frequency-offset optical phase-locked loop (PLL).

A broad spectrum of lasers has been stabilized, from early experiments with gas lasers (He–Ne, CO_2, Ar^+, etc.), to more recent tunable dye lasers, optically pumped solid-state lasers (Ti:sapphire, YAG, etc.) and diode lasers. Usually one or several atomic or molecular transitions are located within the tuning range of the laser to be stabilized. The use of molecular ro-vibrational lines for laser stabilization has been very successful in the infrared using molecules such as CH_4, CO_2, and OsO_4.[10] Their natural linewidths range below 1 kHz, limited by molecular fluorescent decay. Usable linewidths are usually $\geqslant$10 kHz due to the transit of molecules through the light beam. Transitions to higher levels of these fundamental rovibrational states, usually termed overtone bands, extend these rovibrational spectra well into the visible with similar ~kHz potential linewidths. Until recently, the rich spectra of the molecular overtone bands have not been adopted as suitable frequency references in the visible due to their small transition strengths.[11] However, with one of the most sensitive absorption techniques, which combines frequency modulation with cavity enhancement, an excellent S/N for these weak but narrow overtone lines can be achieved,[12] enabling the use of molecular overtones as standards in the visible.[13,14]

Systems based on cold absorber samples potentially offer the highest quality optical frequency sources, mainly due to the drastic reductions of linewidth and velocity-related systematic errors. For example, a few Hz linewidth on the optical transition of Hg^+ was recently observed at the National Institute of Standards and Technology (NIST).[3] Current activity on single ion systems includes Sr^+,[15] Yb^+,[16,17] and In^+.[18] One of the early NIST proposals of using atomic fountains for optical frequency standards[19] has resulted in investigation of the neutral atoms Mg,[20] Ca,[21] Sr,[22,23] Ba,[24] and Ag.[25] These systems could offer ultimate frequency standards free from virtually all of the conventional shifts and broadenings, to the level of one part in 10^{16}–10^{18}. Considerations of a practical system must always include its cost, size, and degree of complexity. Compact and low cost systems can be competitive even though their performance may be 10-fold worse compared with the ultimate system. One such system is Nd:YAG laser stabilized on HCCD at 1064 nm or on I_2 (after frequency doubling) at 532 nm, with a demonstrated stability level of 4×10^{-15} at 300 s averaging time.[26,27] In Fig. 1 we summarize some of the optical frequency standards that are either established or under active development. Also indicated is the spectral width of currently available optical frequency combs generated by mode-locked lasers.

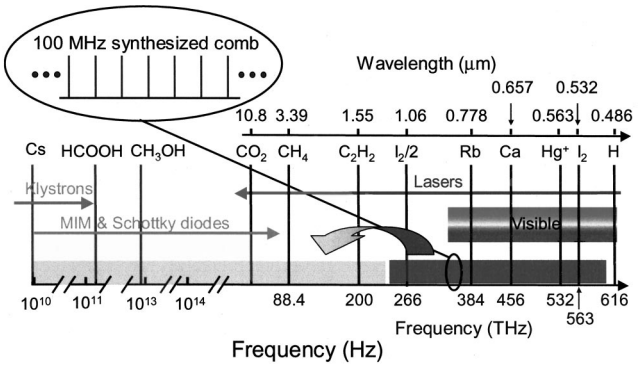

FIG. 1. Map of the electromagnetic spectrum showing frequencies of several atomic and molecular reference transitions and the frequency ranges of sources. Spanning the frequency difference from Cs to the visible portion of the spectrum is now facilitated by the use of femtosecond lasers. The frequency comb generated by mode-locked femtosecond lasers spans the visible and can be transferred to the infrared by difference-frequency generation (shown by the large arrow).

Accurate knowledge of the center of the resonance is essential for establishing standards. Collisions, electromagnetic fringe fields, residual Doppler effects, probe field wavefront curvature, and probe power can all produce undesired center shifts and linewidth broadening. Other physical interactions, and even distortion in the modulation wave form, can produce asymmetry in the recovered signal line shape. For example, in frequency modulation spectroscopy, residual amplitude modulation introduces unwanted frequency shifts and instability and therefore needs to be controlled.[28] These issues must be addressed carefully before one can be comfortable talking about accuracy. A more fundamental issue related to time dilation of the reference system (the second order Doppler effect) can be solved in a controlled fashion, one simply knows the sample velocity accurately (for example, by velocity selective Raman process), or the velocity is brought down to a negligible level using cooling and trapping techniques.

B. Application of standards

The technology of laser frequency stabilization has been refined and simplified over the years and has become an indispensable research tool in many modern laboratories involving optics. Research on laser stabilization has been and still is pushing the limits of measurement science. Indeed, a number of currently active research projects on fundamental physical principles greatly benefit from stable optical sources and need continued progress on laser stabilization. They include laser testing of fundamental principles,[29] gravitational wave detection,[30] quantum dynamics,[31] searching for drift of the fundamental constants,[32–34] atomic and molecular structure, and many more. Recent experiments with hydrogen atoms have led to the best reported value for the Rydberg

constant and $1S$-Lamb shift.[35,36] Fundamental physical constants such as the fine-structure constant, ratio of Planck's constant to electron mass, and the electron-to-proton mass ratio are also being determined with increasing precision using improved precision laser tools.[37] Using extremely stable phase-coherent optical sources, we are entering an exciting era when picometer resolution can be achieved over a million kilometer distance in space. In time keeping, an optical frequency clock is expected to eventually replace the current microwave atomic clocks. In length metrology, the realization of the basic unit, the ''meter,'' relies on stable optical frequencies. In communications, optical frequency metrology provides stable frequency/wavelength reference grids.[38]

A list of just a few examples of stabilized continuous wave (cw) tunable lasers includes millihertz linewidth stabilization (relative to a cavity) for diode-pumped solid state lasers, tens of millihertz linewidth for Ti:sapphire lasers, and subhertz linewidths for diode and dye lasers. Tight phase locking between different laser systems can be achieved,[39] even for diode lasers that have fast frequency noise.

C. Challenge of optical frequency measurement and synthesis

Advances in optical frequency standards have resulted in the development of absolute and precise frequency measurement capability in the visible and near-infrared spectral regions. A frequency reference can be established only after it has been phase coherently compared and linked with other standards. As mentioned above, until recently optical frequency metrology has been restricted to the limited set of ''known'' frequencies, due to the difficulty in bridging the gap between frequencies and the difficulty in establishing the ''known'' frequencies themselves.

The traditional frequency measurement takes a synthesis-by-harmonics approach. Such a synthesis chain is a complex system that involves several stages of stabilized transfer lasers, high-accuracy frequency references (in both optical and rf ranges), and nonlinear mixing elements. Phase-coherent optical frequency synthesis chains linked to the cesium primary standard include Cs–HeNe/CH_4 (3.39 μm)[40,41] and Cs–CO_2/OsO_4 (10 μm).[42] Extension to HeNe/I_2 (576 nm)[43] and HeNe/I_2 (633 nm)[44,45] lasers made use of one of these reference lasers (or the CO_2/CO_2 system[40]) as an intermediate. The first well-stabilized laser to be measured by a Cs-based frequency chain was the HeNe/CH_4 system at 88 THz.[40] With interferometric determination of the associated wavelength[46] in terms of the existing wavelength standard based on krypton discharge, the work led to a definitive value for the speed of light, soon confirmed by other laboratories using many different approaches. Redefinition of the unit of length by adopting $c = 299\,792\,458$ m/s became possible with the extension of the direct frequency measurements to 473 THz (HeNe/I_2 633 nm system) 10 years later by a NIST 10-person team, thus creating a direct connection between the time and length units. More recently, with improved optical frequency standards based on cold atoms (Ca) (Ref. 47) and single trapped ions (Sr^+),[15] these traditional frequency chains have demonstrated measurement uncertainties at the 100 Hz level.

Understandably, these frequency chains are large scale research efforts that require resources that can be provided by only a few national laboratories. Furthermore, the frequency chain can only cover some discrete frequency marks in the optical spectrum. Difference frequencies of many THz could still remain between a target frequency and a known reference. These three issues have represented major obstacles to making optical frequency metrology a general laboratory tool. Several approaches have been proposed and tested as simple, reliable solutions for bridging large optical frequency gaps. Some popular schemes include frequency interval bisection,[48] optical-parametric oscillators (OPO),[49] optical comb generators,[50,51] sum-and-difference generation in the near infrared,[52] frequency division by three-,[53,54] and four-wave mixing in laser diodes.[55] All of these techniques rely on the principle of difference-frequency synthesis, in contrast to the frequency harmonic generation method normally used in traditional frequency chains. In Sec. III we briefly summarize these techniques, their operating principles, and applications. Generation of wide bandwidth optical frequency combs has provided the most direct and simple approach among these techniques and it is the main topic of this review article.

III. TRADITIONAL APPROACHES TO OPTICAL FREQUENCY SYNTHESIS

Although the potential for using mode-locked lasers in optical frequency synthesis was recognized early,[56] these lasers did not provide the properties necessary for fulfilling this potential until recently. Consequently, an enormous effort was invested over the last 40 years in ''traditional'' approaches, which typically involve phase coherently linked single frequency lasers. Traditional approaches to optical frequency measurement can be divided into two subcategories, one is synthesis by harmonic generation, and the other is difference-frequency synthesis. The former method has a long history of success, at the expense of massive resources and system complexity. The latter approach has been the focus of recent research that has led to systems that are more flexible, adaptive, and efficient. Indeed, the main subject of our article, the technique of a wide bandwidth optical frequency comb generator, belongs to the category of difference-frequency generation. For a historical perspective and to have a direct comparison between the two approaches, we first describe the optical frequency chain based on ''classic'' harmonic generation.

A. Phase coherent chains: Traditional frequency harmonic generation

The traditional frequency measurement takes a synthesis-by-harmonic approach. Harmonics, i.e., integer multiples, of a standard frequency are generated with a nonlinear element and the output signal of a higher-frequency oscillator is phase coherently linked to one of the harmonics. Tracking and counting of the beat note, or the use of a PLL, preserves the phase coherence at each stage. Such a phase-coherent frequency multiplication process is continued to

higher and higher frequencies until the measurement target in the optical spectrum is reached. In the frequency region of microwave to midinfrared, a harmonic mixer can perform frequency multiplication and frequency mixing/phase comparison all by itself. ''Cat's whisker'' W–Si point contact microwave diodes, metal–insulator–metal (MIM) diodes, and Schottky diodes have been used extensively for this purpose. In the near infrared to the visible (<1.5 μm), the efficiency of MIM diodes decreases rapidly. Optical nonlinear crystals are better for harmonic generation in these spectral regions. Fast photodiodes perform frequency mixing (nonharmonic) and phase comparison. Such a synthesis chain is a complex system that involves several stages of stabilized transfer lasers, high-accuracy frequency references (in both optical and rf ranges), and nonlinear mixing elements. An important limitation is that each oscillator stage employs different lasing transitions and different laser technologies, so that reliable and cost effective designs are elusive.

1. Local oscillators and phase-locked loops

The most important issue in frequency synthesis is the stability and accuracy associated with such frequency transfer processes. Successful implementation of a synthesis chain requires a set of stable local oscillators at various frequency stages. Maintaining phase coherence across the vast frequency gaps covered by the frequency chain demands that phase errors at each synthesis stage be eliminated or controlled. A more stable local oscillator offers a longer phase coherence time, making frequency/phase comparison more tractable and reducing phase errors accumulated before the servo can decisively express control. Due to the intrinsic property of the harmonic synthesis process, there are two mechanisms responsible for frequency/phase noise entering the loop and limiting the ultimate performance. The first is additive noise, where a noisy local oscillator compromises the information from a particular phase comparison step. The second, and more fundamental one, is the phase noise associated with the frequency (really phase) multiplication process: the phase angle noise increases as the multiplication factor, hence the phase noise spectral density of the output signal from a frequency multiplier increases as the square of the multiplication factor and so becomes progressively worse as the frequency increases in each stage of the chain. Low phase noise microwave and laser local oscillators are therefore important in all PLL frequency synthesis schemes.

The role of the local oscillator in each stage of the frequency synthesis chain is to take the phase information from the lower frequency regions and pass it on to the next level, with appropriate noise filtering, and to reestablish a stable amplitude. The process of frequency/phase transfer typically involves PLLs. Sometimes a frequency comparison is carried out with a frequency counter that measures the difference in cycle numbers between two periodic signals within a predetermined time period. An intrinsic time domain device used to measure zero crossings, e.g., a frequency counter, is sensitive to signal, and noise, in a large bandwidth and so can easily accumulate counting errors resulting from an insufficient signal-to-noise ratio. Even for a PLL, the possibility of cycle slipping is a serious issue. With a specified signal to noise ratio and control bandwidth, one can estimate the average time between successive cycle slips and thus know the expected frequency counting error. For example, a 100 kHz measurement bandwidth requires a signal-to-noise ratio of 11 dB to achieve a frequency error of 1 Hz (1 cycle slip per 1 s).[57]

One function of PLLs is to regenerate a weak signal from a noisy background, thus providing spectral filtering and amplitude stabilization. This function is described as a ''tracking filter.'' Within the correction bandwidth, the tracking filter frequency output follows the perceived rf input sine wave's frequency. A voltage-controlled oscillator (VCO) provides the PLL's constant output amplitude, the variable output frequency is guided by the correction error generated from the phase comparison with the weak signal input. A tracking filter, consisting of a VCO under PLL control, is essential for producing reliable frequency counting, with the regenerated signal able to support the unambiguous zero-crossing measurement for a frequency counter.

2. Measurements made with phase-coherent chains

As described in Sec. III C, only a few phase-coherent optical frequency synthesis chains have ever been implemented. Typically, some important infrared standards, such as the 3.39 μm ($HeNe/CH_4$) system and the 10 μm (CO_2/OsO_4) system, are connected to the Cs standard first. Once established, these references are then used to measure higher optical frequencies.

One of the first frequency chains was developed at the National Bureau of Standards (NBS), and it connected the frequency of a methane-stabilized HeNe laser to the Cs standard.[40] The chain started with a Cs-referenced klystron oscillator at 10.6 GHz, with its seventh harmonic linked to a second klystron oscillator at 74.2 GHz. A HCN laser at 0.89 THz was linked to the 12th harmonic of the second klystron frequency. The 12th harmonic of the HCN laser was connected to a H_2O laser, whose frequency was tripled to connect to a CO_2 laser at 32.13 THz. A second CO_2 laser frequency, at 29.44 THz, was linked to the difference between the 32.13 THz CO_2 laser and the third harmonic of the HCN laser. The third harmonic of this second CO_2 laser finally reached the $HeNe/CH_4$ frequency at 88.3762 THz. The measured value of $HeNe/CH_4$ frequency was later used in another experiment to determine the frequency of an iodine-stabilized HeNe laser at 633 nm, bridging the gap between infrared and visible radiation.[44]

The important 10 μm spectral region covered by CO_2 lasers has been the focus of several different frequency chains.[41,42,58] It is worth noting that in the Whitford chain[58] a substantial number of difference frequencies (generated between various CO_2 lasers) were used to bridge the intermediate frequency gaps, although the general principle of the chain itself is still based on harmonic synthesis. CO_2 lasers provided the starting point of most subsequent frequency chains that reached the visible frequency spectrum.[43,45,59] As noted above, these frequency chains and measurements have led to accurate knowledge of the speed of light, allowing an international redefinition of the ''meter,'' and establishment of many absolute frequency/wavelength standards through-

out the infrared (IR)/visible spectrum. More recently, with improved optical frequency standards based on cold atoms (Ca) (Ref. 47) and single trapped ions (Sr^+),[15] these traditional frequency measurement techniques have demonstrated measurement uncertainties at the 100 Hz level by directly linking the Cs standard to the visible radiation in a single frequency chain.

3. Shortcomings of this traditional approach

It is obvious that such harmonic synthesis systems require a significant investment of human and other resources. The systems need constant maintenance and can be afforded only by national laboratories. Perhaps the most unsatisfying aspect of harmonic chains is that they cover only a few discrete frequency marks in the optical spectrum. Therefore the systems work on coincidental overlaps in target frequencies and are difficult to adapt to different tasks. Another limitation is the rapid increase of phase noise (as n^2) with the harmonic synthesis order (n).

B. Difference-frequency synthesis

The difference-frequency generation approach borrows many frequency measurement techniques developed for the harmonic synthesis chains. Perhaps the biggest advantage of difference-frequency synthesis over the traditional harmonic generation is that the system can be more flexible and compact, and yet have access to more frequencies. We discuss five recent approaches, with the frequency interval bisection and the optical comb generator being the most significant breakthroughs. The common theme of these techniques is the capability to subdivide a large optical frequency interval into smaller portions with a known relationship to the original frequency gap. The small frequency difference is then measured to yield the value of the original frequency gap.

1. Frequency-interval bisection

Bisection of frequency intervals is one of the most important concepts in the difference-frequency generation.[48] Coherent bisection of optical frequency generates the arithmetic average of two laser frequencies f_1 and f_2 by phase locking the second harmonic of a third laser at frequency f_3 to the sum frequency of f_1 and f_2. These frequency-interval bisection stages can be cascaded to provide difference-frequency division by 2^n. Therefore any target frequency can potentially be reached with a sufficient number of bisection stages. Currently the fastest commercial photodetectors can measure heterodyne beats of some tens of GHz. Thus, 6–10 cascaded bisection stages are required to connect a few hundred THz wide frequency interval with a measurable microwave frequency. Therefore the capability of measuring a large beat frequency between two optical signals becomes ever more important, considering the number of bisection stages that can be saved with a direct measurement. A powerful combination is to have an optical comb generator capable of measuring a few THz optical-frequency differences as the last stage of the interval bisection chain. It is worth noting that in a difference-frequency measurement it is typical for all participating lasers to have their frequencies in a nearby frequency interval, thus simplifying system design.

Many optical-frequency measurement schemes have been proposed, and some realized, using interval bisection. The most notable achievement so far has been by Hänsch's group at the Max-Planck Institute for Quantum Optics (MPQ) in Garching. They used a phase-locked chain of five frequency bisection stages to bridge the gap between the hydrogen $1S-2S$ resonance frequency and the 28th harmonic of the HeNe/CH_4 standard at 3.39 μm, leading to improved measurement of the Rydberg constant and the hydrogen ground state Lamb shift.[35] The chain started with a interval divider between a 486 nm laser (one fourth the frequency of the hydrogen $1S-2S$ resonance) and the HeNe/CH_4. The rest of the chain successively reduced the gap between this midpoint near 848 nm and the fourth harmonic of HeNe/CH_4, a convenient spectral region where similar diode laser systems can be employed, even though slightly different wavelengths are required.

2. Optical parametric oscillators

The use of optical parametric oscillators (OPOs) for frequency division relies on parametric down conversion to convert an input optical signal into two coherent subharmonic outputs, the signal and the idler. These outputs are tunable and their linewidths are replicas of the input pump except for the quantum noise added during the down conversion process. The OPO output frequencies, or the original pump frequency, can be precisely determined by phase locking the difference frequency between the signal and the idler to a known microwave or infrared frequency.

In Wong's original proposal, OPO divider stages configured parallel or series were shown to provide the needed multistep frequency division.[49] However, no such cascaded systems have been realized so far, due in part to the difficulty of finding suitable nonlinear crystals for the OPO operation to work in different spectral regions, especially in the infrared. There is progress on the OPO-based optical-frequency measurement schemes, most notably optical-frequency division by 2 and 3,[60,61] that allows rapid reduction of a large frequency gap. Along with threshold-free difference-frequency generations in nonlinear crystals (discussed next), the OPO system provides direct access to calibrated tunable frequency sources in the IR region (20–200 THz).

3. Nonlinear crystal optics

This same principle, i.e., phase locking between the difference frequencies while holding the sum frequency constant, leads to frequency measurement in the near infrared using nonlinear crystals for the sum-and-difference frequency generation. The sum of two frequencies in the near infrared can be matched to a visible frequency standard while the difference matches to a stable reference in the mid-infrared. Another important technique is optical frequency division by 3. This larger frequency ratio could simplify optical frequency chains while providing a convenient connection between visible lasers and infrared standards. An additional stage of mixing is needed to ensure the precise division ratio.[53]

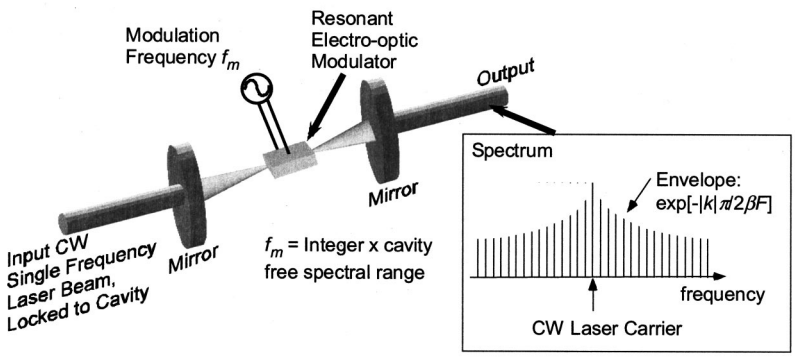

FIG. 2. Schematic of the optical-frequency comb generator based on an intracavity electro-optic modulator. High finesse (typically a few hundred) of the loaded cavity and a large frequency modulation index (β) are instrumental to broad bandwidth of the generated comb (typically a few THz).

4. Four-wave mixing in laser diodes

Another approach to difference-frequency generation relies on four-wave mixing. The idea[55] is to use a laser diode as both a light source and an efficient nonlinear receiver to allow a four-wave mixing process to generate phase-coherent bisection of a frequency interval of a few THz. The setup involves two external cavity diode lasers (ω_{LD1} and ω_{LD2}), separated by 1–2 THz, that are optically injected into a third diode laser for frequency mixing. When the frequency of the third diode laser (ω_{LD3}) is tuned near the interval center of ω_{LD1} and ω_{LD2}, the injection locking mechanism becomes effective and locks ω_{LD3} on the four-wave mixing product, $\omega_{LD1}+\omega_{LD2}-\omega_{LD3}$, leading to the interval bisection condition $\omega_{LD3}=(\omega_{LD1}+\omega_{LD2})/2$. The bandwidth of this process is limited by phase matching in the mixing diode, and was found to be only a few THz.[55]

5. Optical-frequency comb generators

One of the most promising difference-frequency synthesis techniques is the generation of multi-THz optical combs by placing a rf electro-optic modulator (EOM) in a low-loss optical cavity.[50] The optical cavity enhances modulation efficiency by resonating with the carrier frequency and all subsequently generated sidebands, leading to a spectral comb of frequency-calibrated lines spanning a few THz. A schematic of such an optical frequency comb generation process is shown in Fig. 2. The single frequency cw laser is locked onto one of the resonance modes of the EOM cavity, with the free-spectral-range frequency of the loaded cavity being an integer multiple of the EOM modulation frequency. The cavity output produces a comb spectrum with an intensity profile of $\exp(-|k|\pi/\beta F)$,[50] where k is the order of the generated side band from the original carrier, β is the EOM frequency modulation index, and F is the loaded cavity finesse. The uniformity of the comb frequency spacing was carefully verified.[62] These optical frequency comb generators (OFCGs) have produced spectra that extend a few tens of THz,[63] nearly 10% of the optical carrier frequency. At JILA, we developed unique OFCGs, one with the capability of single comb line selection[64] and the other with efficiency enhancement via an integrated OPO/EOM system.[65]

OFCGs had an immediate impact on the field of optical frequency measurement. Kourogi and co-workers[66] produced an optical-frequency map (accurate to 10^{-9}) in the telecommunication band near 1.5 μm using an OFCG that produced a 2 THz wide comb in that wavelength region, connecting various molecular overtone transition bands of C_2H_2 and HCN. The absolute frequency of the Cs D_2 transition at 852 nm was measured against the fourth harmonic of the HeNe/CH_4 standard, with an OFCG bridging the remaining frequency gap of 1.78 THz.[67] At JILA, we used an OFCG to measure the absolute optical frequency of the iodine stabilized Nd:YAG frequency near 532 nm.[27] The level scheme for the measurement is shown in Fig. 3. The sum frequency of a Ti:sapphire laser stabilized on the Rb two photon transition at 778 nm and the frequency-doubled Nd:YAG laser was compared against the frequency-doubled output of a diode laser near 632 nm. The 660 GHz frequency gap between the red diode and the iodine-stabilized HeNe laser at 633 nm was measured using the OFCG.[64]

An OFCG was also used in the measurement of the absolute frequency of a Ne transition ($1S_5 \rightarrow 2P_8$) at 633.6 nm relative to the HeNe/I_2 standard at 632.99 nm.[68,69] The lower level of the transition is a metastable state. Therefore, the resonance can only be observed in a discharged neon cell. The resonance has a natural linewidth of 7.8 MHz. It can be easily broadened (due to unresolved magnetic sublevels) and its center frequency shifted by an external magnetic field. This line is therefore not a high quality reference standard. However, it does have the potential of becoming a low cost

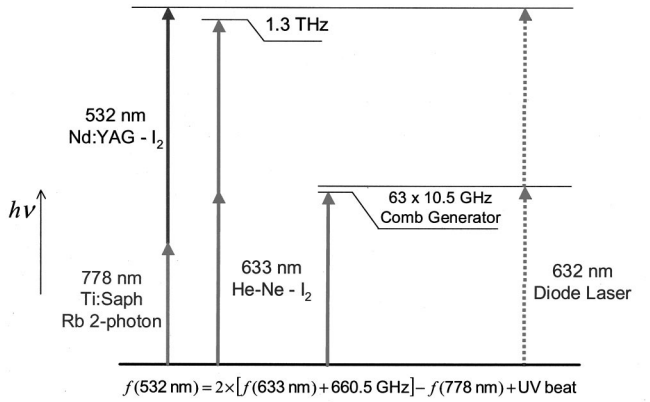

FIG. 3. Measurement of the iodine stabilized Nd:YAG laser frequency using the difference-frequency generation schemes, namely, frequency interval bisection and OFCG. The sum of the frequency of the doubled Nd:YAG laser and a Rb two photon stabilized Ti:S laser at 778 nm is about 1.3 THz higher than the doubled frequency of the iodine-stabilized 633 nm HeNe laser. This frequency gap can be bridged with an optical frequency comb generator based on a 632 nm diode laser (with the gap halved at 660 GHz).

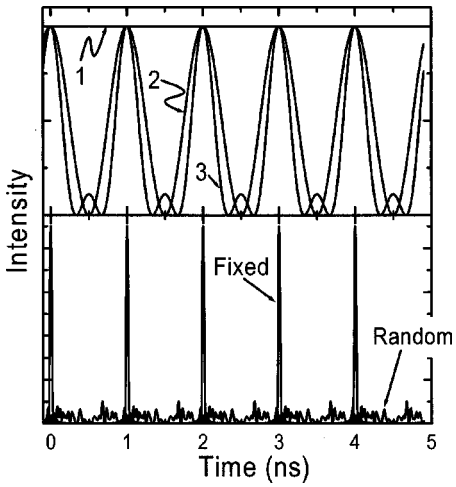

FIG. 4. Schematic of the pulse train generated by locking the phase of simultaneously oscillating modes. The upper panel show the output intensity as the number of modes is increased from 1 to 2 to 3. The lower panel shows the result for 30 modes, both phase locked and with random phases. The mode spacing is 1 GHz.

compact frequency reference that offers frequency calibration on the order of 100 kHz. A red diode laser probe and inexpensive neon lamp form such a system.

The frequency gap between the HeNe/I_2 standard and the neon transition is about 468 GHz, which can easily be measured with an OFCG. The HeNe laser, which is the carrier of the comb, is locked to the $^{127}I_2R(127)11\text{-}5$ component a_{13}. The neon $1S_5 \rightarrow 2P_8$ transition frequency was determined to be 473 143 829.76(0.10) MHz.

The results obtained using OFCGs made the advantages of larger bandwidth very clear. However the bandwidth achievable by a traditional OFCG is limited by cavity dispersion and modulation efficiency. To achieve even larger bandwidth, mode-locked lasers were introduced, thus triggering a true revolution in optical frequency measurement. This is the subject of the remainder of this review article.

IV. MODE-LOCKED LASERS

The OFCGs described above actually generate a train of short pulses. This is simply due to interference among modes with a fixed phase relationship and is depicted in Fig. 4. The first OFCG was built to generate short optical pulses rather than for optical-frequency synthesis or metrology.[70] Later work provided even shorter pulses from an OFCG.[71]

A laser that can sustain simultaneous oscillation on multiple longitudinal modes can emit short pulses; it just requires a mechanism to lock the phases of all the modes, which occurs automatically in an OFCG due to the action of the EOM. Lasers that include such a mechanism are referred to as ''mode locked'' (ML). While the term mode locking comes from this frequency-domain description, the actual processes that cause mode locking are typically described in the time domain.

The inclusion of gain[65,72] and dispersion compensation[73] in OFCGs brings them even closer to ML lasers. The use of ML lasers as optical comb generators has been developed in parallel with the OFCG, starting with the realization that a regularly spaced train of pulses could excite narrow resonances because of the correspondence with a comb in the frequency domain.[74–77] Attention was quickly focused on ML lasers as the source of a train of short pulses.[56,78–93] The recent explosion of measurements based on ML lasers has been largely due to development of the Kerr-lens-mode-locked (KLM) Ti:sapphire laser[94–96] and its capability to generate pulses sufficiently short so that the spectral width approaches an optical octave. In many recent results has been obtained a spectral width exceeding an octave by spectral broadening external to the laser cavity.[89,91,97]

ML lasers have succeeded in generating a much larger bandwidth than OFCGs, which is very attractive. In addition, they tend to be ''self-adjusting'' in the sense that they do not require the active matching between cavity length and modulator frequency that an OFCG does. Although the spacing between the longitudinal modes is easily measured (it is just the repetition rate) and controlled, the absolute frequency positions of the modes is a more troublesome issue and requires some method of active control and stabilization. The incredible advantage of having spectral width in excess of an octave is that it allows the absolute optical frequencies to be determined directly from a cesium clock,[83,89,91] without the need for intermediate local oscillators. Synthesis of optical frequencies directly from a cesium clock can also be accomplished with less than a full optical octave, albeit at the price of a somewhat more complicated apparatus.

In addition to the large bandwidth, ML lasers also have an important advantage over OFCGs with respect to the phase coherence of the modes. In an OFCG, only adjacent modes are phase coherently coupled by the EOM. In a ML laser, the ultrashort pulse results from phase locking of *all* of the lasing modes. This means that there is very strong mutual phase coherence among all of the modes, which is key for the remarkable results obtained using ML lasers for optical-frequency metrology.

A. Introduction to mode-locked lasers

ML lasers generate short optical pulses by establishing a fixed phase relationship among all of the lasing longitudinal modes (see Fig. 4).[98] Mode locking requires a mechanism that results in higher net gain (gain minus loss) for a train of short pulses compared to cw operation. This can be done by an active element, such as an acousto-optic modulator, or passively by saturable absorption (real or effective). Passive ML yields the shortest pulses because, up to a limit, the self-adjusting mechanism becomes more effective than active mode locking, which can no longer keep pace with the ultrashort time scale associated with shorter pulses.[99] Real saturable absorption occurs in a material with a finite number of absorbers, for example, a dye or semiconductor. Real saturable absorption usually has a finite response time associated with relaxation of the excited state. This typically limits the shortest pulse widths that can be obtained. Effective saturable absorption typically utilizes the nonlinear index of refraction of some material together with spatial effects or interference to produce a higher net gain for more intense pulses. The ultimate limit on minimum pulse duration in a ML laser is due to an interplay among the ML mechanism

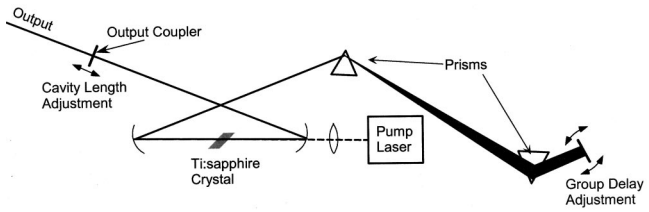

FIG. 5. Schematic of a typical Kerr-lens mode-locked Ti:sapphire laser.

(saturable absorption), group velocity dispersion (GVD), and net gain bandwidth. Strong coupling of the cavity modes is necessary for successfully using mode-locked lasers in optical-frequency synthesis. Mode-locking techniques that utilize essentially instantaneous response, such as the Kerr effect, provide the strongest coupling, and therefore are the preferred technique. The Kerr lens mode-locking technique described below currently dominates the field and provides the characteristics required.

Because of its excellent performance and relative simplicity, the KLM Ti:S laser has become the dominant laser for generating ultrashort optical pulses. A diagram of a typical KLM Ti:S laser is shown in Fig. 5. The Ti:S crystal is pumped by green light from either an Ar^+-ion laser (all lines or 514 nm) or a diode-pumped solid state (DPSS) laser emitting 532 nm. Ti:S absorbs 532 more efficiently, so 4–5 W of pump light is typically used from a DPSS laser, while 6–8 W of light from an Ar^+-ion laser is usually required. The Ti:S crystal provides gain and serves as the nonlinear material for mode locking. The prisms compensate for the group velocity dispersion (GVD) in the gain crystal.[100] Since the discovery of KLM,[94,95] the pulse width obtained directly from the ML laser has been shortened by approximately an order of magnitude by first optimizing the intracavity dispersion[96] and then using dispersion compensating mirrors.[101,102] yielding pulses that are less than 6 fs in duration, i.e., less than two optical cycles. Here we will briefly review how a KLM laser works. While there are other ML lasers and mode-locking techniques, we will not discuss them because of the ubiquity of KLM lasers at the present time. We also note that pulses of similar duration were achieved earlier,[103] however this result relied on external amplification at a low repetition, with pulse broadening and compression, which does not preserve a suitable comb structure for optical-frequency synthesis.

The primary reason for using Ti:S is its enormous gain bandwidth, which is necessary for supporting ultrashort pulses by the Fourier relationship. The gain band is typically quoted as extending from 700 to 1000 nm, although lasing can be achieved well beyond 1000 nm. If this entire bandwidth could be mode locked as a hyperbolic secant or Gaussian pulse, the resulting pulse width would be 2.5–3 fs. While this much bandwidth has been mode locked, the spectrum is far from smooth, leading to longer pulses.

The Ti:S crystal also provides the mode-locking mechanism in these lasers. This is due to the nonlinear index of refraction (Kerr effect), which is manifested as an increase of the index of refraction as the optical intensity increases. Because the intracavity beam's transverse intensity profile is

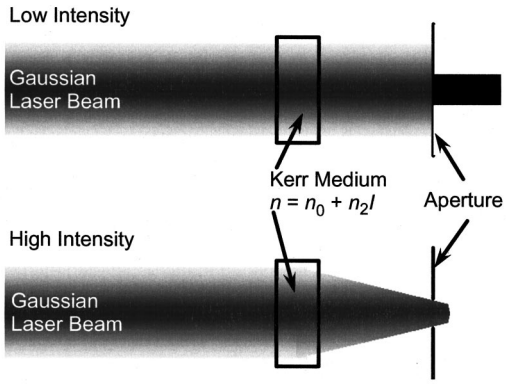

FIG. 6. Schematic of the Kerr-lens mechanism. The upper diagram shows that, for low intensity, much of the intensity does not pass through the aperture. At high intensity, the Gaussian index profile, which is due to the nonlinear index of refraction, acts as a lens and focuses the beam and increases net transmission.

Gaussian, a Gaussian index profile is created in the Ti:S crystal. A Gaussian index profile is equivalent to a lens, hence the beam slightly focuses, with the focusing increasing with increasing optical intensity. Together with a correctly positioned effective aperture, the nonlinear (Kerr) lens can act as a saturable absorber, i.e., high intensities are focused and hence transmit fully through the aperture while low intensities experience losses (see Fig. 6). Since short pulses produce higher peak powers, they experience lower loss, making mode-locked operation favorable. While some KLM lasers include an explicit aperture, the small size of the gain region can act as one. This mode-locking mechanism has the advantage of being essentially instantaneous; no real excitation is created that needs to relax. It has the disadvantages of not being self-starting and of requiring a critical misalignment from optimum cw operation.

Spectral dispersion in the Ti:S crystal due to the variation of the index of refraction with wavelength will result in temporal spreading of the pulse each time it traverses the crystal. At these wavelengths, sapphire displays ''normal'' dispersion, where longer wavelengths travel faster than shorter ones. To counteract this, a prism sequence is used in which the first prism spatially disperses the pulse, causing the long wavelength components to travel through more glass in the second prism than the shorter wavelength components.[100] The net effect is to generate ''anomalous'' dispersion to counteract the normal dispersion in the Ti:S crystal. The spatial dispersion is undone by placing the prism pair at one end of the cavity so that the pulse retraces its path through the prisms. With the optimum choice of material, it is possible to minimize both GVD and third order dispersion, yielding operation that is limited by the fourth order dispersion.[104] It is also possible to generate anomalous dispersion with dielectric mirrors;[105] these are typically called ''chirped mirrors.'' They have the advantage of allowing shorter cavity lengths but the disadvantage of less adjustability if used alone. Also, at present, they are only available from a small number of suppliers. Chirped mirrors also allow additional control over higher order dispersion and have been used in combination with prisms to produce pulses even shorter than those achieved using prisms alone.[101,102]

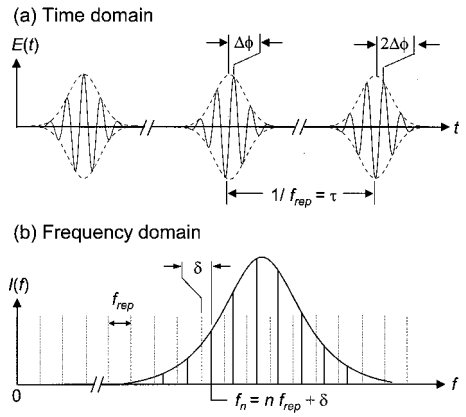

FIG. 7. Time–frequency correspondence between $\Delta\phi$ and δ. (a) In the time domain, the relative phase between the carrier (solid line) and the envelope (dotted line) evolves from pulse to pulse by $\Delta\phi$. Generally, the absolute phase is given by $\phi=\Delta\phi(t/\tau)+\phi_0$, where ϕ_0 is an unknown overall constant phase. (b) In the frequency domain, the elements of the frequency comb of the mode-locked pulse train are spaced by f_{rep}. The entire comb (solid line) is offset from integer multiples (dotted line) of f_{rep} by an offset frequency $\delta=\Delta\phi f_{\mathrm{rep}}/2\pi$. Without active stabilization, δ is a dynamic quantity that is sensitive to perturbation of the laser. Hence $\Delta\phi$ changes in a nondeterministic manner from pulse to pulse in an unstabilized laser.

B. Frequency spectrum of mode-locked lasers

To successfully exploit ML lasers for the generation of frequency combs with known absolute frequencies, it is necessary to understand the spectrum emitted by a mode-locked laser, how it arises, and how it can be controlled. While it is always possible to describe the operation of these lasers in either the time or frequency domain, details of connecting the two are rarely presented.[106] Unless sufficient care is taken, it is easy for misunderstandings to arise when attempting to convert understanding in one domain into the other.

We will start with a time domain description of the pulses emitted by a mode-locked laser. This is shown in Fig. 7(a). The laser emits a pulse every time the pulse circulating inside the cavity impinges on the output coupler. This results in a train of pulses separated by time $\tau=l_c/v_g$ where l_c is the length of the cavity and v_g is the net group velocity. Due to dispersion in the cavity, the group and phase velocities are not equal. This results in a phase shift of the ''carrier'' wave with respect to the peak of the envelope for each roundtrip. We designate the shift between successive pulses as $\Delta\phi$. It is given by

$$\Delta\phi=\left(\frac{1}{v_g}-\frac{1}{v_p}\right)l_c\omega_c \bmod 2\pi,$$

where v_p is the intracavity phase velocity and ω_c is the carrier frequency. This pulse-to-pulse shift is shown in Fig. 7(a). The overall carrier-envelope phase of a given pulse, which obviously changes from pulse to pulse if $\Delta\phi\neq 0$, includes an offset which does not affect the frequency spectrum. We are therefore not concerned with this offset phase here, although it is a subject of current interest in the ultrafast optics community.

1. Comb spacing

The frequency spectrum of the pulse train emitted by a ML laser consists of a comb of frequencies. The spacing of the comb lines [Fig. 7(b)] is simply determined by the repetition rate of the laser. This is easily obtained by Fourier transforming a series of δ-function-like pulses over time. The repetition rate is in turn determined by the group velocity and the length of the cavity.

2. Comb position

If all of the pulses had the same phase relative to the envelope, i.e., $\Delta\phi=0$, then the spectrum is simply a series of comb lines with frequencies that are integer multiples of the repetition rate. However this is not in general true, due to the difference between the group and phase velocities inside the cavity. To calculate the effect of a pulse-to-pulse phase shift on the spectrum, we write the electric field, $E(t)$, of a pulse train. At a fixed spatial location, let the field of a single pulse be $E_1(t)=\hat{E}(t)e^{i(\omega_c t+\phi_0)}$. Then the field for a train of pulses is

$$E(t)=\sum_n \hat{E}(t-n\tau)e^{i(\omega_c t-n\omega_c\tau+n\Delta\phi+\phi_0)}$$

$$=\sum_n \hat{E}(t-n\tau)e^{i(\omega_c t+n(\Delta\phi-\omega_c\tau)+\phi_0)},$$

where $\hat{E}(t)$ is the envelope, ω_c is the carrier frequency, ϕ_0 is the overall phase offset, and τ is the time between pulses (for pulses emitted by a mode-locked laser $\tau=t_g$, where t_g is the group roundtrip delay time of the laser cavity). If we take the Fourier transform, we obtain

$$E(\omega)=\int\sum_n \hat{E}(t-n\tau)e^{i[\omega_c t+n(\Delta\phi-\omega_c\tau)+\phi_0]}e^{-i\omega t}dt$$

$$=\sum_n e^{i[n(\Delta\phi-\omega_c\tau)+\phi_0]}\int \hat{E}(t-n\tau)e^{-i[(\omega-\omega_c)t]}dt,$$

letting $\tilde{E}(\omega)=\int\hat{E}(t)e^{-i\omega t}dt$ and recalling the identity $\int f(x-a)e^{-i\alpha x}dx=e^{-i\alpha a}\int f(x)e^{-i\alpha x}dx$ we obtain

$$E(\omega)=\sum_n e^{i[n(\Delta\phi-\omega_c\tau)+\phi_0]}e^{-in(\omega-\omega_c)\tau}\tilde{E}(\omega-\omega_c)$$

$$=e^{i\phi_0}\sum_n e^{i(n\Delta\phi-n\omega\tau)}\tilde{E}(\omega-\omega_c).$$

The significant components in the spectrum are the ones for which the exponential in the sum add coherently because the phase shift between pulse n and $n+1$ is a multiple of 2π. Equivalently $\Delta\phi-\omega\tau=2m\pi$. This yields a comb spectrum with frequencies

$$\omega_m=\frac{\Delta\phi}{\tau}-\frac{2m\pi}{\tau},$$

or, converting from angular frequency, $f_m=mf_{\mathrm{rep}}+\delta$ where $\delta=\Delta\phi f_{\mathrm{rep}}/2\pi$ and $f_{\mathrm{rep}}=1/\tau$ is the repetition frequency. Hence we see that the position of the comb is offset from integer multiples of the repetition rate by a frequency δ,

which is determined by the pulse-to-pulse phase shift. This is shown schematically in Fig. 7(b). Thus the frequency spectrum of a mode-locked laser is a series of comb lines with frequencies given by

$$f_n = n f_{\mathrm{rep}} + \delta,$$

where n is an integer that indexes the comb lines. This simple equation is the basis for much of what follows.

C. Frequency control of the spectrum

For the comb generated by a ML laser to be useful for synthesizing optical frequencies, control of its spectrum, i.e., the absolute position and spacing of the comb lines, is necessary. In terms of the above description of the output pulse train, this means control of the repetition rate, f_{rep}, and the pulse-to-pulse phase shift, $\Delta\phi$. Once the pulses have been emitted by the laser, f_{rep} cannot be controlled. $\Delta\phi$ can be controlled by shifting the frequency of the comb, for example, with an acoustooptic modulator.[107] However it is generally preferable to control both f_{rep} and $\Delta\phi$ by making appropriate adjustments to the operating parameters of the laser itself. Some experiments only require control of the repetition rate, f_{rep}. This can easily be obtained by adjusting the cavity length using a piezoelectric transducer (PZT) to translate one of the end mirrors. Temperature stabilizing the base plate for the laser reduces cavity length drift and allows an ordinary PZT to achieve sufficient range. PZT stacks can twist as they expand or contract, thereby requiring a more complex arrangement.[108]

Many experiments are simplified by locking both f_{rep} and δ. To do so, both the roundtrip group delay and the roundtrip phase delay must be controlled. Adjusting the cavity length changes both. If we rewrite f_{rep} and δ in terms of roundtrip delays, we find

$$f_{\mathrm{rep}} = \frac{1}{t_g}; \quad \delta = \frac{\omega_c}{2\pi t_g}(t_g - t_p),$$

where $t_g = l_c / v_g$ is the roundtrip group delay and $t_p = l_c / v_p$ is the roundtrip phase delay. Both t_g and t_p depend on l_c, therefore another parameter must be used to control them independently. Methods for doing this will be discussed later. The equation for δ may seem unphysical because it depends on ω_c, which is arbitrary, however there is an implicit dependence on ω_c that arises due to the dispersion in v_p (and hence t_p) that cancels the explicit dependence. Note that v_p must have dispersion for $v_p \neq v_g$ and that v_g must be constant (dispersionless) for stable mode-locked operation.

D. Spectral broadening

It is generally desirable to have a comb that spans the greatest possible bandwidth. At the most basic level, this is simply because it allows measurement of the largest possible frequency intervals. Ultimately, when the output spectrum from a comb generator is sufficiently wide, it is possible to determine the absolute optical frequencies of the comb lines directly from a microwave clock, i.e., without relying on intermediate phase-locked oscillators. The simplest of these techniques requires a spectrum that spans an octave, i.e., the high frequency components have twice the frequency of the low frequency components. In the transform limit and for a spectrum with a single peak, this bandwidth would correspond to a single cycle pulse, which has yet to be achieved at optical frequencies. Thus it has been necessary to rely on external broadening of the spectrum. Fortunately, the optical heterodyne technique employed for detection of single comb components is very sensitive, therefore it is not necessary to have a 3 dB bandwidth of an octave. Detection is typically feasible even when the power at the octave points is 10–30 dB below the peak.

Self-phase modulation (SPM) occurs in a medium with a nonlinear index of refraction, i.e., a third order optical nonlinearity. It generates new frequencies, thereby broadening the spectrum of a pulse. This process occurs in the gain crystal of a ML laser and can result in output spectra that exceed the gain bandwidth. In the frequency domain it can be viewed as four-wave mixing between the comb lines. The amount of broadening increases with the peak power per unit cross-sectional area of the pulse in the nonlinear medium. Consequently, an optical fiber is often used as a nonlinear medium because it confines the optical power into a small area and results in an interaction length that is longer than could be obtained in a simple focus. While the small cross section can be maintained for very long distances, the high peak power in fact is typically only maintained for a rather short distance because of group velocity dispersion in the fiber, which stretches the pulse over time and reduces the peak power. Nevertheless, it has been possible to generate an octave of usable bandwidth with an ordinary single spatial mode optical fiber by starting with very short and intense pulses from a low repetition rate laser.[109] The low repetition rate increases the energy per pulse despite limited average power, thereby increasing the broadening. The fiber was only 3 mm long. The pulses were pre-chirped before being launched into the fiber so that the dispersion in the fiber would recompress them.

The recent development of microstructured fiber has made it possible to easily achieve well in excess of an octave bandwidth using the output from an ordinary KLM Ti:S laser.[97,110] Microstructured fibers consist of a fused silica core surrounded by air holes. This design yields a waveguide with a very high contrast of the effective index of refraction between the core and the cladding. The resultant waveguiding provides a long interaction length with a minimum beam cross section. In addition, the waveguiding permits designing of the zero point of the group velocity dispersion to be within the operating spectrum of a Ti:S laser (for ordinary fiber the group velocity dispersion zero can only occur for wavelengths longer than 1.3 μm). Figure 8 shows the dispersion curves for several different core diameters.[110] This dispersion property means that the pulse does not disperse and the nonlinear interaction occurs over a long distance (centimeters to meters, rather than millimeters in ordinary fiber). Typical input and output spectra are shown in Fig. 9. The output spectrum is very sensitive to the launched power and polarization. It is also sensitive to the spectral position relative to the zero-GVD point and the chirp of the incident pulse. Because the fiber displays anomalous dispersion, pre-compensation of

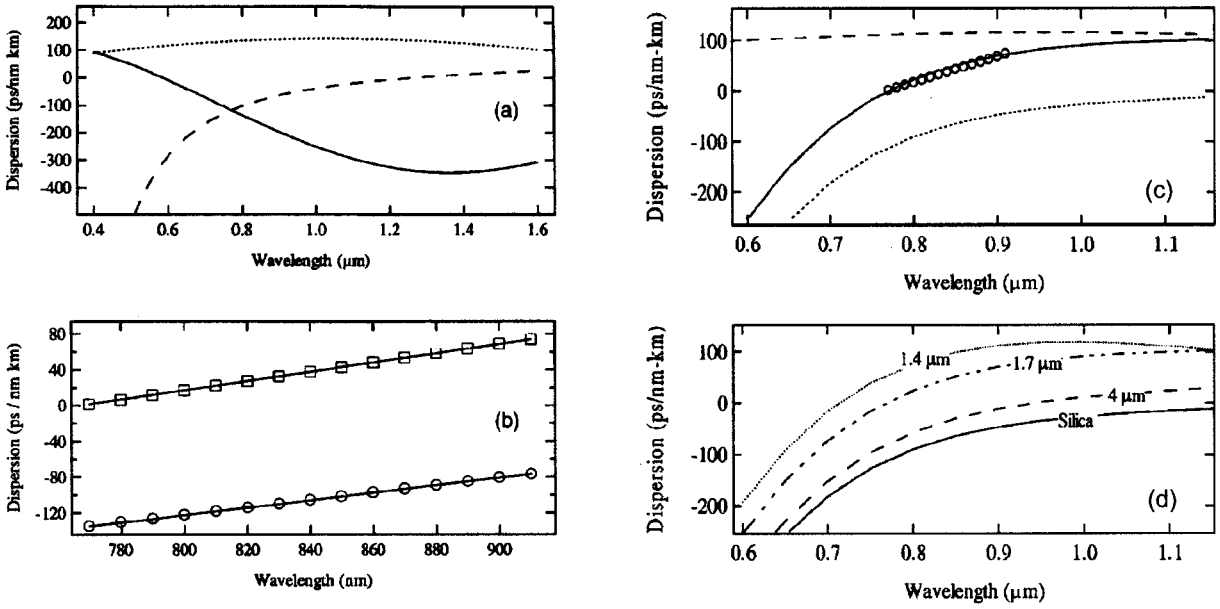

FIG. 8. Properties of the microstructure fiber. (a) Calculated group velocity dispersion for a silica fiber with a core-cladding index difference of 0.1 and a core diameter of 1 μm (solid curve) and a fiber with a core-cladding index difference of 0.3 and a core diameter of 2 μm (dotted curve). The GVD of bulk silica is shown by the dashed curve. (b) Measured GVD of the microstructure fiber (squares) and standard single mode fiber (circles). (c) Calculated waveguide GVD contribution (dashed line), material dispersion of bulk silica (dotted curve), and resulting net GVD (solid) curve of the microstructure fiber. Experimentally measured values from (b) are shown by circles. (d) Calculated net GVD of the microstructure fiber as the fiber dimensions are scaled for 1.4, 1.7, and 4 μm core diameters. (Reproduced from Refs. 97 and 110 with permission of the authors.)

the dispersion is not required if the laser spectrum is centered toward the long wavelength side of the zero-GVD point (i.e., in the anomalous dispersion region). Because the pulse is tuned close to a zero-GVD point, the output phase profile is dominated by third order dispersion.[111]

Nonlinear processes in the microstructure fiber also produce broadband noise in the radio-frequency spectrum of a photodiode that detects the pulse train. This has deleterious effects on the optical-frequency measurements described below because the noise can mask the heterodyne beats [see Fig. 10(c)]. The noise increases with increasing input pulse energy and appears to display threshold behavior.[112] This makes it preferable to use short input pulses since less broadening, and hence less input power, is required. The exact origin of the noise is currently uncertain, but it may be due to guided acoustic-wave Brillouin scattering,[113–115] Raman scattering, or modulation instabilities. This problem can be overcome by increasing the resolution of the detection system.

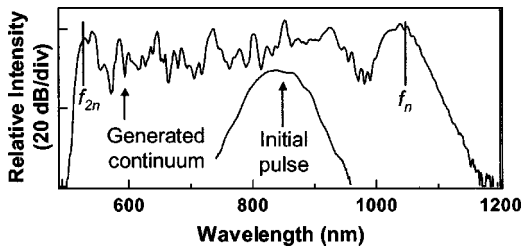

FIG. 9. Continuum generation by and air–silica microstructured fiber. Self-phase modulation in the microstructured fiber broadens the output of the laser so that is spans more than one octave. The spectra are offset vertically for clarity.

V. OPTICAL-FREQUENCY MEASUREMENTS USING MODE-LOCKED LASERS

Optical frequency measurements are typically made to determine the absolute optical frequency of an atomic, molecular, or ionic transition. Typically, a single frequency laser is locked to an isolated transition, which may be among a rich manifold of transitions, and then the frequency of the single frequency laser is measured. Mode-locked lasers are

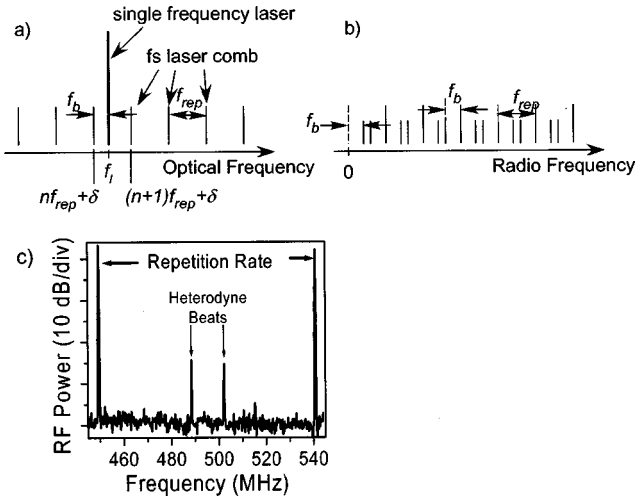

FIG. 10. Correspondence between optical frequencies and heterodyne beats in the rf spectrum. (a) Optical spectrum of a mode-locked laser with mode spacing $f_{\rm rep}$ plus a single frequency laser at frequency f_l. (b) Detection by a fast photodiode yields a rf spectrum with equally spaced modes due to the mode-locked laser (long lines) plus a pair of intervening beats signals due to heterodyning (short lines). (c) Typical experimental rf spectrum showing both repetition rate beats and heterodyne beats.

typically employed in measurement of the frequency of the single frequency laser. This is performed by heterodyning the single frequency laser against nearby optical comb lines of the mode-locked laser. The resulting heterodyne rf signal (see Fig. 10) contains beats at frequencies $f_b = |f_l - nf_{\mathrm{rep}} - \delta|$ where f_l is the frequency of the single frequency laser, f_{rep} the repetition rate of the ML laser, n an integer, and δ the offset frequency of the ML laser (see Sec. I B 2). This yields, in the rf output of a photodetector, a pair of beats within every rf frequency interval between mf_{rep} and $(m+1)f_{\mathrm{rep}}$. One member of the pair arises from comb lines with $nf_{\mathrm{rep}} > f_l$ and the other from lines with $nf_{\mathrm{rep}} < f_l$. Both the beat frequencies and f_{rep} can be easily measured with standard rf equipment. Typically, f_{rep} itself is not measured, but rather one of its harmonics (10th to ~100th harmonic), to yield a more accurate measurement in a given measurement time since the uncertainty is divided by the harmonic number. More sophisticated techniques can yield even greater precision in the measurement of f_{rep} and can, in addition, allow comparison of the stability of two optical frequencies independent of f_{rep}.[116] To map from these beat frequency measurements to the optical frequency f_l, we need to know n and δ. Since n is an integer, we can estimate it if we have previous knowledge about f_l to within $\pm f_{\mathrm{rep}}/4$. Typically f_{rep} is greater than 80 MHz, putting this requirement easily in the range of commercially available wave meters, which have an accuracy of ~25 MHz. Alternatively, n can be determined by dithering f_{rep} and analyzing the resulting changes in the optical beat note. Thus, measurement of δ is the remaining problem. This can be done by comparison of the comb to an intermediate optical-frequency standard, which is discussed in Sec. V B, or directly from the microwave cesium standard as will be described below. Several such techniques for direct links between microwave and optical frequencies are described in Sec. V C.

A. Locking techniques

Although measurement of f_{rep} and δ are in principle sufficient to determine an absolute optical frequency, it is generally preferable to use the measurements in a feedback loop to actively stabilize or lock one or both of them to suitable values. If this is not done, then they must be measured simultaneously with each other and with f_b to obtain meaningful results. In Sec. III, we described the physical quantities in the laser that determine f_{rep} and δ. Here we describe the technical details of adjusting these physical quantities.

The cavity length is a key parameter for locking the comb spectrum. It is useful to examine a specific example of the sensitivity to the length. Consider a laser with a repetition rate of 100 MHz and a center wavelength of 790 nm (~380 THz). The repetition rate corresponds to a cavity length of 1.5 m which is 3.8 million wavelengths long (roundtrip). A length decrease of $\lambda/2$ gives an optical-frequency shift of exactly one order, +100 MHz, for all of the optical-frequency components. The corresponding shift of the 100 MHz repetition rate is $(100\,\mathrm{MHz})/(380\,\mathrm{THz}) = +2.63 \times 10^{-7}$ fractionally or +26.31 Hz. Since the cavity length is most sensitive to environmental perturbations on both fast (vibrations) and slow (temperature) time scales, good control of it warrants close attention. Furthermore, we note that length variations have a much larger effect on the optical frequency of a given comb line than on the repetition rate.

Since the adjustment and locking of two quantities, f_{rep} and δ, are desired, a second parameter in addition to the cavity length must be controlled. We will present details of using the swivel angle of the back mirror to obtain the desired degree of freedom.[85] This is the mostly widely implemented and the one with which we are most familiar. We will show that the swivel angle changes the group delay, which would lead one to believe that it should be used to control f_{rep}. However, we will also show that δ does not depend on l_c. Thus, it is necessary to control f_{rep} by adjusting l_c and δ by the swivel angle. This is counterintuitive, and occurs because in order for a change in the swivel angle to leave the frequency of a given optical mode constant (i.e., as a fixed point in the comb spectrum) it must change δ to compensate for the change in f_{rep}.

We note that the language of ''fixed points'' in the comb spectrum, introduced by Telle, can also be very useful in discussing the combined action of various control parameters on the comb spectrum.[117] This yields insight into optimum control strategies and noise contributions.

1. Comb spacing

The comb spacing is given by $f_{\mathrm{rep}} = 1/t_g = v_g/l_c$, where v_g is the roundtrip group velocity and l_c is the cavity length. The simplest way of locking f_{rep} is by adjusting l_c. Mounting either end mirror in the laser cavity on a translating piezo-electric actuator easily does this (see Fig. 5). The actuator is typically driven by a phase-locked loop that compares f_{rep} or one of its harmonics to an external clock. For an environmentally isolated laser, the short time jitter in f_{rep} is lower than in most electronic oscillators, although f_{rep} drifts over long times. Thus the locking circuit needs to be carefully designed for a sufficiently small bandwidth so that f_{rep} does not have fast noise added while its slow drift is being eliminated.

Locking the comb spacing alone is sufficient for measurements that are not sensitive to the comb position such as measurement of the frequency difference between two lasers (f_{L1} and f_{L2}). For example, suppose the frequency of f_{L1} is higher than its beating comb line, while f_{L2} is lower than its corresponding comb line. The sum of these two beats is taken using a double-balanced mixer, the resulting sum frequency is $f_s = f_{\mathrm{L1}} - nf_{\mathrm{rep}} - \delta - (f_{\mathrm{L2}} - mf_{\mathrm{rep}} - \delta) = (f_{\mathrm{L1}} - f_{\mathrm{L2}}) - (m-n)f_{\mathrm{rep}}$. Where $nf_{\mathrm{rep}} + \delta < f_{\mathrm{L1}}$ and $mf_{\mathrm{rep}} + \delta > f_{\mathrm{L2}}$, a minus sign arises due to the absolute value in determining the beat frequencies (see the expression for f_b above). If f_{L1} and f_{L2} are known with accuracy better than $f_{\mathrm{rep}}/2$, then $(m-n)$ can be determined and hence $f_{\mathrm{L1}} - f_{\mathrm{L2}}$ from f_s.

2. Comb position

The frequency of a given comb line is given by $f_n = nf_{\mathrm{rep}} + \delta$, where n is a large integer. This means that simply changing the cavity length can control the frequency of comb lines. However, this also changes the comb spacing, which is undesirable if a measurement spans a large number of comb lines. Controlling δ instead of f_{rep} allows a rigid

shift of the comb positions, i.e., the frequency of all the lines can be changed without changing the spacing.

The comb position depends on the phase delay, t_p, and the group delay, t_g. Each delay in turn depends on the cavity length. In addition, the comb position depends on the carrier frequency, which is determined by the lasing spectrum. To obtain independent control of both the comb spacing and position, an additional parameter, besides the cavity length, must be adjusted.

A controllable group delay is produced by a small rotation about a vertical axis (swivel) of the end mirror of the laser in the arm that contains the prisms (see Fig. 5). This is because the different spectral components are spread out spatially across the mirror. The dispersion in the prisms results in a linear relationship between the spatial coordinate and the wavelength. Hence the mirror swivel provides a linear phase with frequency, which is equivalent to a group delay.[118] The group delay depends linearly on the angle for small angles. If the pivot point for the mirror corresponds to the carrier frequency, then the effective cavity length does not change. The angle by which the mirror is swiveled is very small, approximately 10^{-4} rad. If we assume that swiveling the mirror only changes the group delay by an amount $\alpha\theta$, where θ is the angle of the mirror and α is a constant that depends on the spatial dispersion on the mirror and has units of s/rad, then we rewrite

$$f_{\mathrm{rep}}=\frac{1}{l_c/v_g+\alpha\theta};\quad \delta=\frac{\omega_c}{2\pi}\left(1-\frac{l_c/v_p}{(l_c/v_g)+\alpha\theta}\right).$$

From these equations we can derive how the comb frequencies depend on the control parameters, l_c and θ. To do so we will need the total differentials

$$\begin{aligned} df_{\mathrm{rep}}&=\frac{\partial f_{\mathrm{rep}}}{\partial\theta}d\theta+\frac{\partial f_{\mathrm{rep}}}{\partial l_c}dl_c\\ &=-\frac{\alpha}{(l_c/v_g+\alpha\theta)^2}d\theta-\frac{1/v_g}{(l_c/v_g+\alpha\theta)^2}dl_c\\ &\cong-\alpha\frac{v_g^2}{l_c^2}d\theta-\frac{v_g}{l_c^2}dl_c,\\ d\delta&=\frac{\omega_c}{2\pi}\frac{l_c\alpha}{v_p}\frac{1}{[(l_c/v_g)+\alpha\theta]^2}d\theta\\ &\quad-\frac{\omega_c}{2\pi}\frac{\alpha\theta/v_p}{[(l_c/v_g)+\alpha\theta]^2}dl_c\\ &\cong\frac{\omega_c}{2\pi}\frac{v_g^2\alpha}{v_p l_c}d\theta, \end{aligned}$$

where the final expressions are in the approximation that $\alpha\theta\ll l_c/v_g$. From this, we see that δ is controlled solely by θ. The concomitant change in f_{rep} can be compensated for by changes in the cavity length.

Physically, we can understand these relationships by considering how the optical frequencies of individual modes depend on the length and swivel angle. This is shown schematically in Fig. 11 for an example of a 1 cm long cavity. From the upper part it is clear that the dominant effect of changing the cavity length is the position change of each optical mode, the repetition rate (spacing between modes) changes much less, by a ratio of the repetition rate/optical frequency. Thus the change in the repetition rate is only apparent for larger changes in the length (cf. the left and right upper panels in Fig. 11). This is because the repetition rate is multiplied by the mode number to reach the optical frequency. Swiveling the mirror does not change the frequency of the mode at the pivot point (mode 10 005 in the lower panel of Fig. 11), but causes the adjacent modes to move in opposite directions. This can be understood in terms of a frequency dependent cavity length, in this example it increases for decreasing frequencies.

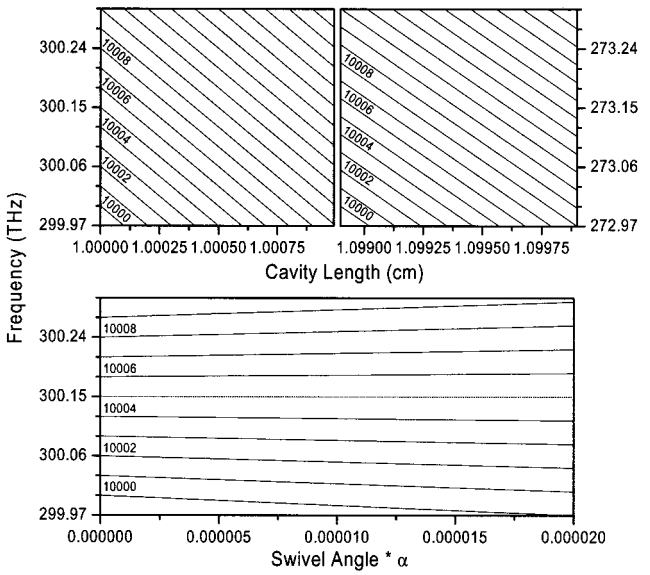

FIG. 11. Schematic showing how the modes of a cavity depend on the cavity length (upper panels) and swivel angle of the mirror behind the prisms. For illustrative purposes, a 1 cm cavity was used. Comparison of the left and right upper panels shows the weak dependence of the mode spacing on cavity length.

3. Comb position and spacing

It is often desirable to simultaneously control/lock both the comb position and spacing, or an equivalent set of parameters, say, the position of two comb lines. In an ideal situation, orthogonal control of f_{rep} and δ may be desirable to allow the servo loops to operate independently. If this cannot be achieved, one servo loop will have to correct changes made by the other. This is not a problem if they have very different response speeds. If their responses are similar, interaction between loops can lead to problems, including oscillation. If necessary, orthogonalization can be achieved by either mechanical design in some cases, or by electronic means in all cases.

Note that we earlier assumed that the pivot point of the tilting mirror corresponds to the carrier frequency. This is overly restrictive, because moving the pivot point will give an additional parameter that can be adjusted to help orthogonalize the parameters of interest. We can generalize our treatment to include an adjustable pivot point by allowing l_c to depend on θ. The resulting analysis shows that it is impossible to orthogonalize δ and f_{rep} by a simple choice of the

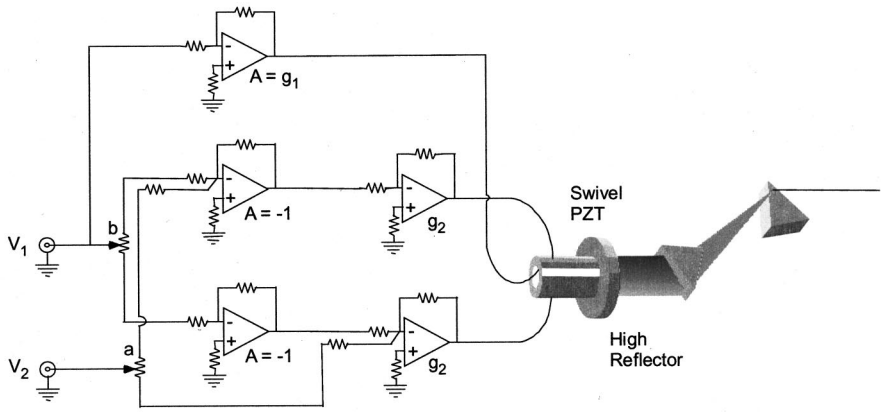

FIG. 12. Schematic of a circuit that actuates the length-swivel PZT based on two error signal inputs (V_1 and V_2). The circuit allows an appropriate admixture to be generated by adjusting the potentiometers, labeled by *a* and *b*.

pivot point. Further examination of the lower panel in Fig. 11 makes it clear why this must be so. The comb line at (or near) the pivot point does not change its frequency when the swivel angle changes. This is inconsistent with being able to control δ while holding f_{rep} constant, which is equivalent to a rigid shift of all of the comb lines (none are constant, therefore there can be no pivot point).

Although we cannot orthogonalize δ and f_{rep} by choosing a pivot, the analysis does show how to do so, we merely need to make the length change of the cavity proportional to the swivel angle. This can be implemented electronically and amounts to inverting the linear matrix equation connecting $d\delta$ and df_{rep} to $d\theta$ and dl_c. An electronic remedy also addresses the practical issue that experimental error signals generated to control the comb often contain a mixture of two degrees of freedom. For example, the two error signals can correspond to the position of a single comb line (usually with respect to a nearby single frequency laser) and the comb spacing. A more interesting situation is when the error signals correspond to the position of two comb lines. Typically, this will be obtained by beating a comb line on the low frequency side of the spectrum with a single frequency laser and a comb line on the high frequency side with the second harmonic of the single frequency laser. In both of these cases, the error signals contain a mixture of δ and f_{rep}, which in turn are determined by a mixture of the control parameters l_c and θ.

As will be evident below, having a pair of error signals that correspond to the positions of two comb lines is the most interesting.[119] This is obtained by beating the two comb lines against two single frequency lasers with frequencies f_{L1} and f_{L2}. The beat frequencies are given by $f_{bi}=f_{\mathrm{L}i}-(n_i f_{\mathrm{rep}}+\delta)$ with $i=1, 2$ (for clarity we have assumed that $f_{\mathrm{L}i}$ is above the nearest comb line with index n_i). Taking the differentials of these equations and inverting the result we obtain

$$df_{\mathrm{rep}}=\frac{df_{b1}-df_{b2}}{n_2-n_1}\rightarrow\frac{1}{n}(df_{b1}-df_{b2}),$$

$$d\delta=\frac{n_1/n_2 df_{b2}-df_{b1}}{1-n_1/n_2}\rightarrow df_{b2}-2df_{b1},$$

where the expressions after the arrows are for $f_{b2}=2f_{b1}$, i.e., we are using the fundamental and second harmonics of a single laser with *n* being the index of the laser comb mode just below the fundamental frequency. These equations can be combined with those connecting $d\delta$ and df_{rep} to $d\theta$ and dl_c to obtain

$$d\theta=\frac{2\pi v_p l_c}{\omega_c v_g^2\alpha}(df_{b2}-2df_{b1}),$$

$$dl_c=-\frac{l_c^2}{v_g n}[(1-2An)df_{b1}+(An-1)df_{b2}],$$

$$A=\frac{2\pi v_p}{\omega_c l_c}.$$

These equations directly connect the observables with the control parameters for this configuration (note that the product *An* is of the order of 1). Equations of similar form have been derived without determining the values of the coefficients.[119]

It is desirable to design an electronic orthogonalization circuit that is completely general. Although we have expressions telling us what the coefficients connecting the observables and control parameters should be, we typically do not know the values of all of the parameters that appear in the coefficients. Furthermore, there may be technical factors that cause unwanted mixing of the control parameters or error signals that must be compensated for. Such coupling arises, for example, because the two transducers have differing frequency response bandwidths. Finally, a general circuit can readily be adapted to experimental configurations other than the one discussed in detail above.

The electronic implementation depends on the actuator mechanisms. We employed a piezoelectric transducer tube in which application of a transverse (between the inside and outside of the tube) voltage results in a change of the tube length. By utilizing a split outer electrode, the PZT tube can be made to bend in proportion to the voltage difference between the two outer electrodes. The common mode voltage, or the voltage applied to the inner electrode, causes the PZT to change its length, which we will designate ''piston'' mode. Mounting the end mirror of the laser cavity on one end of the PZT tube allows it to be both translated and swiveled, which corresponds to changing the cavity length (l_c) and the mirror angle (θ).

The circuit shown in Fig. 12 allows a mixture of two

error inputs to be applied to both the piston and swivel modes of the mirror. The coefficients a and b are adjusted via the potentiometers where the neutral midpoints correspond to $a=b=0$ and more generally

$$a,b \propto \frac{R_{\mathrm{up}}-R_{\mathrm{low}}}{R_{\mathrm{up}}+R_{\mathrm{low}}},$$

where R_i represents the resistance above or below the feedpoint. The gains of the amplifiers, g_1 and g_2, provide additional degrees of freedom. The length and swivel angle are related to the input voltages by

$$\begin{aligned} l_c &\propto g_1 V_1 + g_2 V_1 - g_2 a V_2 \\ \theta &\propto 2 g_2 (b V_1 + V_2) \end{aligned} \qquad -1 < a,b < 1.$$

Thus if $a=b=0$, then l_c only responds to V_1 and θ only responds to V_2. By adjusting a,l_c can be made to also respond to V_2, with either sign, this is also the case for b and V_1.

4. Other control mechanisms

In addition to tilting the mirror after the prism sequences, the difference between the group and phase delays can also be adjusted by changing the amount of glass in the cavity[120] or adjusting the pump power.[120,121]

The amount of glass can be changed by moving a prism or by introducing glass wedges. Changing the amount of glass changes the difference between the group delay and phase delay due to dispersion in the glass. It has the disadvantage of also changing the effective cavity length. Furthermore, rapid response time in a servo loop cannot be achieved because of the limitation of mechanical action on the relatively high mass of the glass prism or wedge.

Changing the pump power changes the power of the intracavity pulse. This has empirically been shown to change the pulse-to-pulse phase.[120] Intuitively, it might be expected that this would lead to a change in the nonlinear phase shift experienced by the pulses as they traverse the crystal. However, a careful derivation shows that the group velocity also depends on the pulse intensity in such a way as to mostly cancel out the phase shift.[122] Thus it is not too surprising that the correlation between power and phase shift is the opposite of what is expected from this simple picture.[120] The phase shift is attributed to the shifting of the spectrum that accompanies changing the power. This will yield a changing group delay due to group velocity dispersion in the cavity. Such an effect is similar to the control of θ. Nevertheless, it is possible to achieve very tight locking due to the much larger servo bandwidth afforded by an optical modulator compared to physically moving an optical element.[121] Although the servo loop stabilizes the frequency spectrum of the mode-locked laser, it also reduces amplitude noise, presumably because amplitude noise is converted into phase noise by nonlinear processes in the laser. More work is needed to fully understand the mechanism and to exploit it for control of the comb.

Frequency shifts of the comb have also been obtained by focusing light from a diode laser into the Ti:sapphire crystal.[123] The diode laser light depletes the gain, thereby altering the intracavity intensity and thus changing the nonlinear phase shift. High modulation bandwidth can also be obtained using this technique.

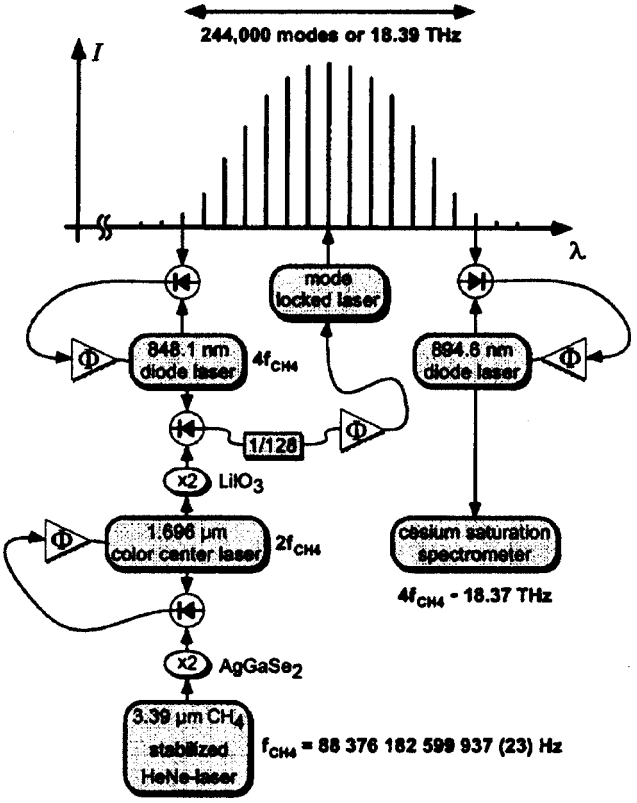

FIG. 13. Schematic of the frequency chain used to measure the frequency of the cesium D_1 line using a mode-locked laser. The methane-stabilized HeNe laser served as an intermediate. (Reproduced from Ref. 85 with permission of the authors.)

The offset frequency of the comb can also be controlled externally to the laser cavity by using and acouto-optic modulator. This has been exploited to lock the comb to a reference cavity.[107]

B. Measurements using an intermediate reference

The simplest use of the frequency comb from a mode-locked laser is to measure the frequency difference between two optical sources, typically single frequency lasers. If the absolute optical frequency of one of the two sources is known, this yields an absolute measurement of the other. This strategy had been demonstrated by Kourogi and coworkers using the OFCG described in Sec. III B 5.[66] In Secs. V B1, V B2, and VC, we present two representative recent examples of such measurements based on wider combs generated by ML lasers.

1. Cesium D_1 line

One of the first measurements to utilize the broadband comb from a KLM Ti:S laser was performed by Hänsch's group at MPQ.[85] This experiment measured the absolute frequency of the cesium D_1 line and was, we believe, the first that utilized phase coherent control of the position of a femtosecond laser comb. The KLM Ti:S laser generated 73 fs pulses and was used as part of a complex frequency chain (see Fig. 13) that connected a 3.39 μm CH_4 stabilized HeNe

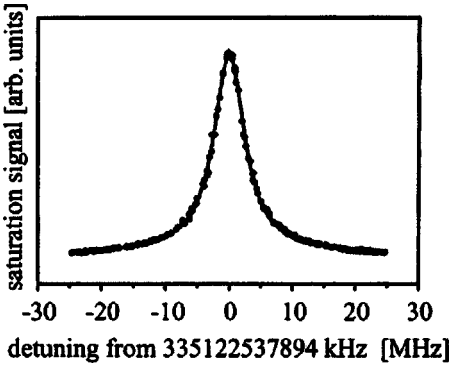

FIG. 14. $F_g=4\rightarrow F_e=4$ component of the Cs D_1 transition. The absolute frequency is determined from the fitted Lorentzian (solid line). (Reproduced from Ref. 85 with permission of the authors.)

laser at 88.4 THz to a laser locked on the cesium D_1 line via a saturation spectrometer. The KLM Ti:S laser spanned the 18.4 THz gap between the fourth harmonic of the HeNe laser (353.5 THz) to the frequency of the cesium D_1 line of 335.1 THz. The HeNe laser was transportable and its absolute frequency had been measured earlier at the Physikalisch-Technische Bundesanstalt (PTB) in Braunschweig using their traditional frequency chain starting from the microwave cesium clock. The MPQ frequency chain involved a color center laser operating at 1696 nm and two diode lasers at 848.1 and 894.1 nm. Four phase-locked loops were required to lock the lasers and the femtosecond comb. Only the position of the comb was controlled, not the spacing (repetition rate), which was simply measured to determine the frequency interval. The experiment yields results[85] (see Fig. 14) with an accuracy that was three orders of magnitude better than previous measurements. When combined with other measurements, it provided a new determination of the fine structure constant.

2. Measurement across 104 THz

The measurements described above stimulated intense interest in the optical frequency metrology community. Clearly the goal was to increase the frequency gap that could be spanned using a ML laser. This led to work at JILA that demonstrated measurement across 104 THz.[88] This was

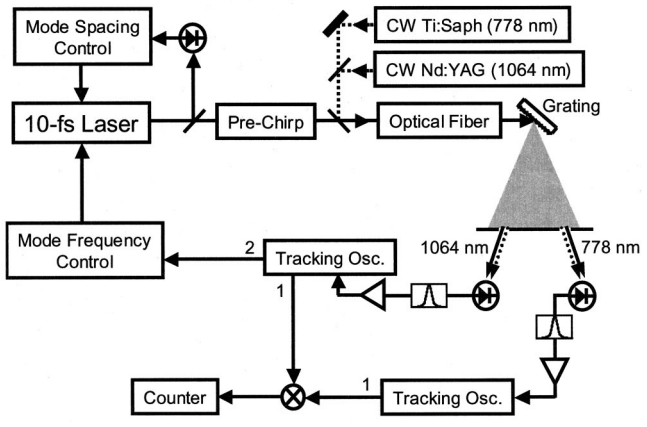

FIG. 15. Experimental setup used to bridge the 104 THz gap between I_2-stabilized Nd:YAG and Rb-stabilized Ti:sapphire single frequency lasers.

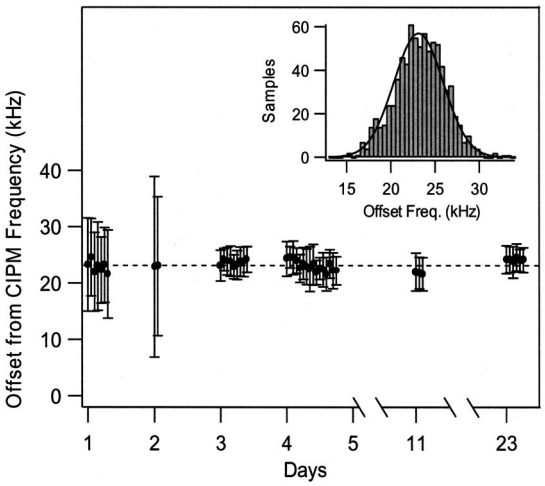

FIG. 16. Measured Nd:YAG frequency with respect to the CIPM recommended value of 281 630 111 740 kHz. The dashed line is the average of all plotted points (23.2 kHz). The inset is a histogram of the ~800 individual measurements on the third day. Note that direct measurement of our Rb standard (Fig. 18) reveals it to be -3.7 ± 5 kHz relative to the CIPM recommended value.

achieved by starting with a laser that generated pulses approximately 10 fs in duration (see Fig. 15). The already broad spectrum of these pulses was further increased by self-phase modulation in standard single mode optical fiber (SMF). The usable width of the resulting spectrum was approximately 165 THz. One side of the 104 THz gap that was measured was the frequency of the $5S_{1/2}(F=3)\rightarrow 5D_{5/2}(F=5)$ two photon transition of ^{85}Rb at 778 nm. A single frequency Ti:S laser was locked to this transition. The other side of the gap was a single frequency Nd:YAG laser at 1064 nm that had its second harmonic locked to the a_{10} component of the $R(56)32\text{-}0$ transition in $^{127}I_2$. The 778 nm laser served as a known reference, with a Comité International des Poids et Mesures (CIPM) recommended uncertainty of only ±5 kHz. The measurement yielded an improved measurement of the frequency of the 1064 nm laser (Fig. 16) which had a CIPM recommended uncertainty of ±20 kHz. The results yielded an offset of 23.1 kHz from the CIPM recommended value with a measurement uncertainty of ±2.8 kHz, with additional ±5 kHz uncertainty due to the 778 nm standard. This experiment began the present epoch in which the measurement inaccuracy is less than that of the available standards, due to femtosecond lasers.

C. Direct optical to microwave synthesis

While the measurements described above showed the promise of the large bandwidth comb generated by a femtosecond ML laser, it quickly became clear that it was possible to use them to measure optical frequencies directly from the microwave primary standard for frequency. There are several techniques for doing this,[83] depending on how much bandwidth is generated by the ML laser. The simplest of these requires a spectrum that spans a full octave, i.e., because the blue end of the spectrum is twice the frequency of the red end. Although a ML laser that directly generates an octave of spectrum has very recently been reported,[124] all of the fre-

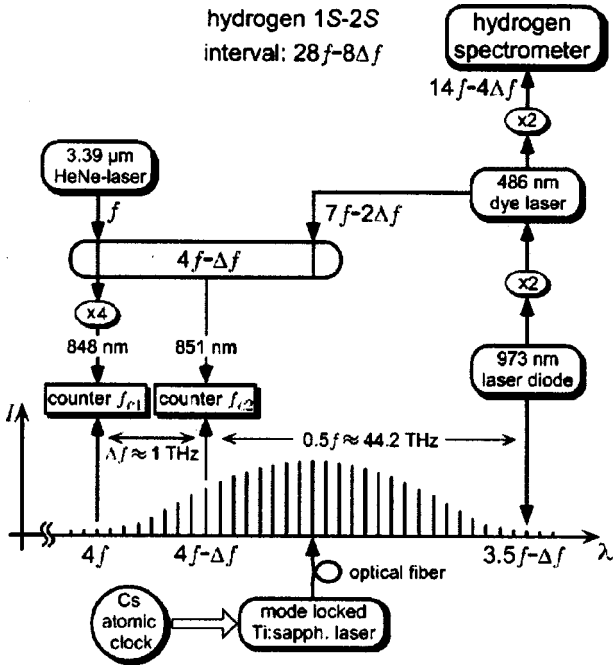

FIG. 17. Frequency chain used to simultaneously measure the frequency of the hydrogen $1S-2S$ transition and that of a methane stabilized HeNe laser. (Reproduced from Ref. 92 with permission of the authors.)

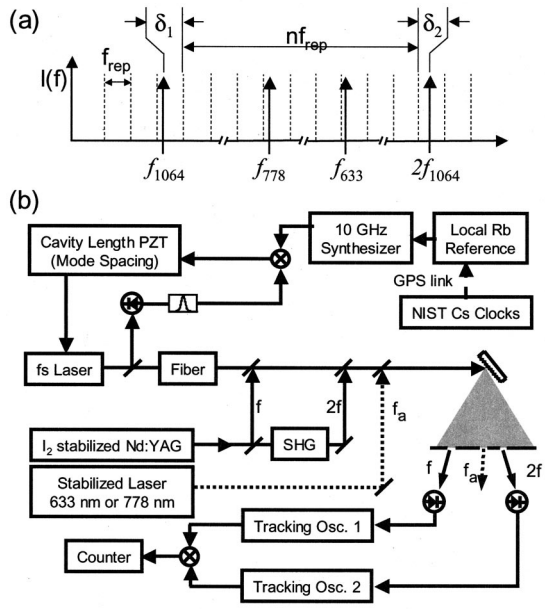

FIG. 18. Direct measurement of the absolute frequency of an I_2-stabilized Nd:YAG laser. The only input is a microwave clock. (a) Relationship between the single frequency laser (f_{1064}), its second harmonic ($2\,f_{1064}$), the comb from the mode-locked laser (dashed lines) and the measured heterodyne beats, δ_1 and δ_2. Also shown are frequencies of the Rb-stabilized Ti:sapphire laser (f_{778}) and I_2-stabilized HeNe (f_{633}) measured in a second experiment. (b) Schematic of the setup.

quency measurements so far have used external broadening of the spectrum to achieve the full octave (see Sec. III D). In the following we describe three measurements that utilize a full octave. We also describe an important measurement that used a more complex chain with several bisection stages so that a full octave was not necessary.

1. Methane stabilized HeNe and hydrogen $1S-2S$ transition with bisection

The first experiment to utilize a mode-locked laser to make absolute optical frequency measurements referenced directly to a microwave clock was performed at MPQ.[92] This experiment simultaneously measured the frequency of a methane stabilized HeNe laser and the $1S-2S$ interval in hydrogen. Without an octave spanning mode-locked laser, it required a more complex frequency chain than the techniques described in the following. The chain included five phase-locked intermediate oscillators and a single bisection stage (see Fig. 17). It used the mode-locked laser comb to span the frequency intervals between $4f$ and $4f-\Delta f$ and between $4f-\Delta f$ and $3.5f-\Delta f$, where $f\sim 88.4$ THz is the frequency of the HeNe laser and Δf is chosen so that $28f-8\Delta f$ is the frequency of the H $1S-2S$ transition. The repetition rate of the mode-locked laser was locked to a cesium atomic clock. Note that measurement of the interval $4f-\Delta f$ to $3.5f-\Delta f$ yields $0.5f$ and hence f itself.

Later work by the same group compared the results of this chain with and $f-2\,f$ chains (described below).[121] The results put an upper limit of 5.1×10^{-16} on the uncertainty of the new $f-2\,f$ chains.

2. I_2 stabilized Nd:YAG by $f-2\,f$

Given an octave spanning frequency comb and the output of a stabilized single frequency laser, the frequency of the single frequency laser can be determined by measuring the frequency interval between the laser and its second harmonic, i.e., $2\,f-f=f$, where f is the frequency of the single frequency laser. This technique requires the least amount of effort to control the comb, only the comb spacing needs to be controlled. In principle, the comb spacing does not have to be locked, it only needs to be measured. Of course, that will add uncertainty to the final frequency measured if the measurement intervals are not exactly coincident due to gating of the counters. As described in Sec. V A1, if the beat frequencies are chosen so that the frequency difference between f and a lower frequency comb line is measured at the same time the frequency difference between $2\,f$ and a higher frequency comb line is measured and the appropriate difference or sum taken, the absolute frequency position of the comb is canceled and does not enter into the final measurement [see Fig. 18(a)]. This means that the comb position does not need to be controlled and any change in it does not matter as long as it occurs on a time scale that is slow compared to the speed with which the differencing occurs. This is easily achieved by heterodyning the two beat signals [see Fig. 18(b)].

This technique was utilized at JILA to make one of the first direct microwave to optical measurements using a single mode-locked laser.[91] In this experiment the octave spanning frequency spectrum was obtained by spectral broadening in a piece of microstructured optical fiber.[97,110] The results yielded a frequency for the a_{10} component of the $R(56)32\text{-}0$ transition of $^{127}I_2$ 34.4 kHz higher than the recommended

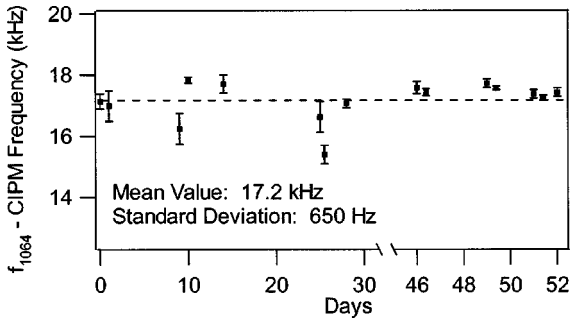

FIG. 19. Summary of direct rf to optical measurement of $f1064$ plotted with respect to the CIPM recommended value. The $+17.2$ kHz average of all measurements is shown by the dashed line.

CIPM value (see Fig. 19). The standard deviation was 1.3 kHz. Including uncertainty in the realization of the a_{10} frequency, the final value reported was $563\,260\,223\,514 \pm 5$ kHz.

3. Rb stabilized Ti:sapphire and I_2 stabilized HeNe by Nd:YAG $f-2f$

Once the absolute frequency of a stabilized single frequency laser is known by using an octave spanning comb, it can be used as a ''reference'' and the frequency of any other comb line determined. This allows it to be used to measure the frequency of any other source that lies within the frequency span of the comb. This concept was utilized to measure the frequency of a Ti:sapphire laser stabilized to the $5S_{1/2}(F=3)\rightarrow 5D_{5/2}(F=5)$ two photon transition in ^{85}Rb and that of a HeNe laser stabilized to the a_{13} component of transition 11-5,$R(127)$ of $^{127}I_2$ (peak i).[91] Both measurements yield results with uncertainties of one part in 10^{11} or better. The measurement of the metrologically important 633 nm HeNe laser was carried one step further when an international intercomparison was made between the absolute measurement using the JILA femtosecond comb and a traditional frequency chain maintained at the National Research Council of Canada.[125] This time the 633 nm laser was locked to the f peak of the I_2 spectrum. The agreement between the JILA and NRC measurements was 220 ± 770 Hz, yielding a measurement accuracy of 1.6×10^{-12}. Such frequency intercomparison between different laboratories using different technologies often reveals and permits studies of systematic errors of either locking or frequency measurement techniques.

Further work showed that the dominant source of instability in these measurements was actually the microwave reference oscillator used to lock the comb spacing.[119] The fact that optical frequencies are $\sim 3\times 10^6$ times the repetition rate means that the frequency instability in the microwave source gets amplified by a similar factor. This was ascertained by locking the frequency between the fundamental of a Nd:YAG laser and the nearest comb line with a phase-locked loop. The uncertainty in the apparent position of the other comb lines was shown to increase with the frequency separation from the locked line. In general these results show that for short times the mode-locked laser is very stable, but it drifts over longer times, necessitating the use of an external reference.

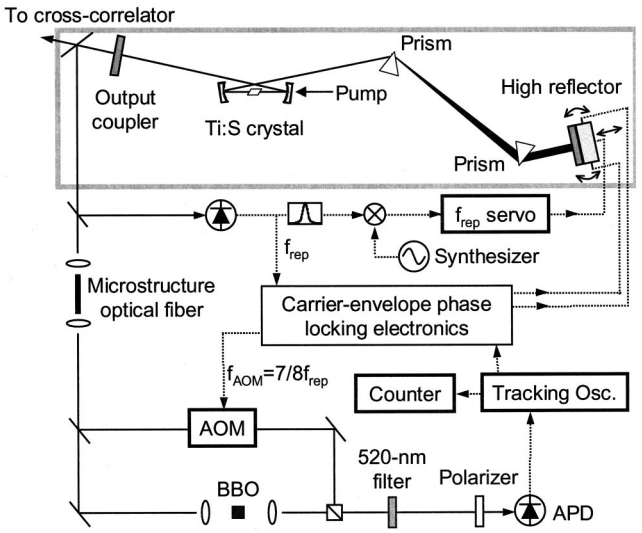

FIG. 20. Schematic of the self-referenced synthesizer. Solid lines represent optical paths and dashed lines are electrical connections.

4. Self-referenced synthesizer

Direct optical synthesis from a microwave clock is possible using only a single mode-locked laser without an auxiliary single frequency laser. This is done by directly frequency doubling the long wavelength portion (near frequency f) of the octave-spanning spectrum and comparing it to the short wavelength side (near frequency $2f$). Thus it requires more power in the wings of the spectrum produced by the femtosecond laser than if an auxiliary single frequency cw laser were used. However, the fact that many comb lines contribute to the heterodyne signal means that a strong beat signal can be obtained even if the doubled light is weak.

This technique was first demonstrated at JILA by Jones *et al.*[89] A diagram of the experiment is shown in Fig. 20. The octave-spanning spectrum is again obtained by external broadening in microstructure fiber. The output is spectrally separated using a dichroic mirror. The long wavelength portion is frequency doubled using a β-barium-borate crystal. Phase matching selects a portion of the spectrum near 1100 nm for doubling. The short wavelength portion of the spectrum is passed through an acoustooptic modulator (AOM). The AOM shifts the frequencies of all of the comb lines. This allows the offset frequency, δ, to be locked to zero, which would not otherwise be possible due to degeneracy in the rf spectrum between the $f-2f$ heterodyne beat signal and the repetition rate comb. The resulting heterodyne beat directly measures δ and is used in a servo loop to fix the value of δ. The repetition rate is also locked to an atomic clock. The end result is that the absolute frequencies of all of the comb lines are known to within an accuracy limited only by the rf standard.

The resulting comb was then used to measure the frequency of a 778 nm single frequency Ti:sapphire laser that was locked to the $5S_{1/2}(F=3)\rightarrow 5D_{5/2}(F=5)$ two photon

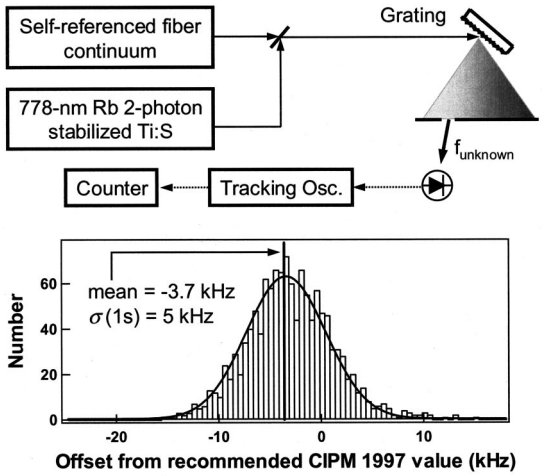

FIG. 21. Frequency measurement using the self-referenced comb. The diagram shows the experimental setup for measuring the two photon transition in ^{85}Rb using the self-referenced comb.

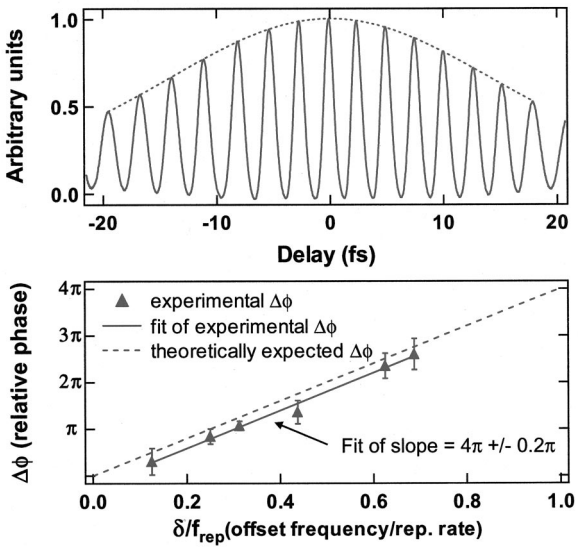

FIG. 22. Time–domain cross correlations. The upper panel shows a typical cross correlation between pulse i and pulse $i+2$ emitted from the laser along with the fit of the envelope. The relative phase is extracted by measuring the difference between the peak of the envelope and the nearest fringe. This is plotted in the lower panel as a function of locking frequency (relative to the repetition rate). The linear fit produces the expect slope of 4π with a small overall phase shift that is attributed to the correlator.

transition in ^{85}Rb. This was done by combining the comb with the single frequency laser using a 50–50 beamsplitter [see Fig. 21(a)]. A small portion of the spectrum near 778 nm is selected and the beat between the comb and the single frequency laser measured. A histogram of the measured frequencies is shown in Fig. 21. Averaging over several days yielded a value of -4.2 ± 1.3 kHz compared to the CIPM recommended value. This agrees quite well with the measurement described in section VC3 for the same Rb system.

5. Recent measurements

As this review article is being written, many more measurements are being performed and reported. The rapid pace of advancement guarantees that any list will be out of date by the time of publication. A very important set of measurements, which warrants notice, is being made of candidates for use as optical clocks. These include a single Hg^+ ion and calcium in a magneto-optic trap. A single trapped Hg^+ ion recently yielded[3] the narrowest optical resonance ever observed, with a width of only 6.7 Hz, equivalent to $Q\sim1.4\times10^{14}$. This incredibly narrow line greatly reduces the uncertainty in the measurement of the frequency, which was recently done using a mode-locked laser.[126] The results yielded an uncertainty of ~3 Hz, making it the most precise optical measurement to date. A mode-locked laser has also been used to measure the frequency interval between the frequencies of the Hg^+ ion and trapped Ca atoms.[127] The frequency of Ca has also been measured at PTB using a femtosecond laser directly.[128] Other high precision measurements published during the last year include those of single Yb (Ref. 116) and In (Ref. 129) ions.

VI. OUTLOOK

In the last 2 years we have seen remarkable advances in the field of optical frequency synthesis and metrology, with femtosecond mode-locked lasers becoming a truly powerful tool for optical frequency synthesis and metrology. The vast simplification that results from using femtosecond lasers is making optical frequency metrology a routine laboratory technique, as opposed to an enterprise that requires enormous effort and expense. This paradigm shift is demonstrated by the large number of results using femtosecond lasers that have been already been reported in the last few months.

Here in Sec. VI we will briefly discuss some issues that appear to be important in the future.

A. Time domain implications

As described in Sec. III, frequency offset arises from the pulse-to-pulse shift of the carrier-envelope phase. Thus controlling the frequency offset is equivalent to controlling the pulse-to-pulse phase shift. This has been shown experimentally by cross correlation (see Fig. 22). It is the first step towards controlling the carrier-envelope phase of ultrafast pulses (not just the pulse-to-pulse phase change). The carrier-envelope phase is expected to affect extreme nonlinear optics, for example, x-ray generation.[130] As discussed below, the overall carrier-envelope phase is also manifest in coherent control experiments where interference between different orders occurs.

If an experimental technique can be developed that is sensitive to the carrier-envelope phase and works with the direct output of a mode-locked oscillator (i.e., without that amplification that will be necessary for extreme nonlinear optics), it may in turn benefit optical-frequency synthesis because it may create a simpler technique for determining/controlling the comb offset frequency.

B. Higher repetition rate

Increasing the repetition rate of the mode-locked laser is beneficial because it increases the comb spacing. This increases the power in each individual comb line, which makes

the heterodyne signals with a single frequency laser stronger. It also makes it easier to separate out the beat signal amongst the forest of comb lines and it reduces the requirements on *a priori* knowledge of the frequency of a source. A Kerr-lens mode-locked ring laser was demonstrated that achieves repetition rates of 2 GHz.[131] This laser uses dispersion-compensating mirrors, rather than a prism sequence. This necessitates the use of an alternate technique for control of the comb, such as ''servoing'' the pump power. Versions of this laser have been used in measurements.[121] Note, for a given average power, high repetition rates correspond to a lower pulse energy, which reduces the external nonlinear spectral broadening. Thus we expect that there is a maximum useful repetition rate.

C. Direct generation of an octave

Most rf to optical-frequency synthesizers based on mode-locked lasers reported to date use microstructured fiber to broaden the output spectrum of the laser so that it spans a full octave. While this has proven to be an effective technique, it would clearly be simpler if an octave could be generated directly from a mode-locked laser. Obtaining an octave directly from the laser would also mitigate concerns about phase noise generated in the fiber used to broaden the spectrum. It might seem impossible for a Ti:sapphire laser to generate such a broad spectrum due to the limited gain bandwidth of Ti:sapphire of ~300 nm. However lasers have often been observed to generate spectral components outside of the gain region. This is due to self-phase modulation in the gain crystal. Recently Ell *et al.*[124] reported the generation of an octave directly from a laser by including a second waist in the laser cavity. A glass plate is positioned at the second waist, thereby yielding additional self-phase modulation. This laser employed special pairs of double-chirped mirrors so that a time focus occurred at the second waist.[132]

D. High precision atomic and molecular spectroscopy and coherent control

A phase stable femtosecond comb represents a major step towards ultimate control of light fields as a general laboratory tool. Many dramatic possibilities are ahead. For high resolution laser spectroscopy, the precision-frequency comb provides a tremendous opportunity for improved measurement accuracy. For example, in molecular spectroscopy, different electronic, vibrational, and rotational transitions can be studied simultaneously with phase coherent light of various wavelengths, leading to determination of molecular structure and dynamics with unprecedented precision. For sensitive absorption spectroscopy, multiple absorption or dispersion features can be mapped efficiently with coherent multiwavelength light sources. A phase-coherent wide-bandwidth optical comb can also induce the desired multipath quantum interference effect for a resonantly enhanced two photon transition rate.[93] This effect can be understood equally well from the frequency domain analysis and time domain Ramsey-type interference. The multipulse interference in the time domain gives an interesting variation and generalization of the two-pulse-based temporal coherent control of the excited state wave packet.

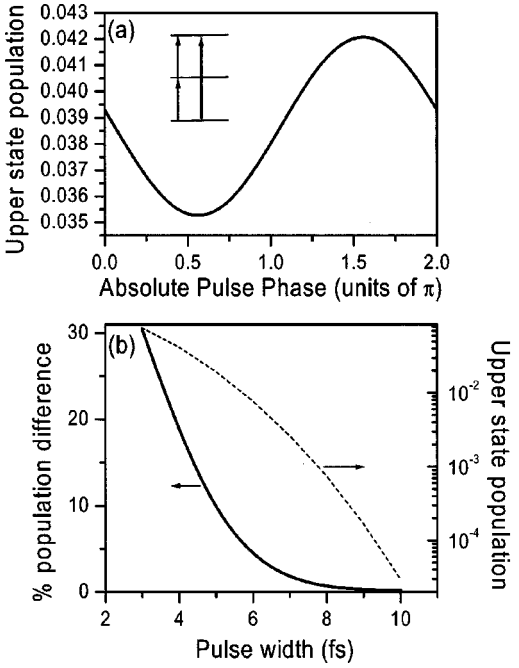

FIG. 23. Results of a simple simulation showing that the upper state population of the three-level system is sensitive to the absolute pulse phase if the upper state can be reached by both single photon and two photon pathways. The phase dependence is shown in (a) and the dependence on the pulse width is shown in (b).

Stabilization of the relative phase between the pulse envelope and the optical carrier should lead to more precise control of the pulse shape and timing, and open the door for many interesting experiments in the areas of extreme nonlinear optics and quantum coherent control. The first step towards coherent control of a chemical reaction is selective excitation of atomic or molecular excited state populations. This is usually achieved by controlling the *relative* phase of pairs or multiplets of pulses. If the phase of the pulse(s) that arrive later in time is the same as the excited state–ground state atomic phase, the excited state population is increased, whereas if the pulse is antiphased, the population is returned to the ground state. With ultrashort pulses, it is possible to achieve *single pulse* coherent control by interference between pathways of different nonlinear order, for example, between three photon and four photon absorption. Such interference between pathways is sensitive to the absolute phase. This has been discussed for multiphoton ionization.[133] For a pulse with a bandwidth that is close to spanning an octave, interference between one and two photon pathways will be possible, thereby lessening the power requirements. A simulation of this is shown in Fig. 23(a), where the upper state population is plotted as a function of absolute phase for the ideal three-level system, shown in the inset. In Fig. 23(b), the dependence on pulse width is shown. The effect is measurable for pulses that are far from spanning an octave. However real atoms do not have perfectly spaced levels, which will reduce the effect, and this simple simulation ignores selection rules.

E. Optical clocks

Measurement of absolute optical frequencies has suddenly become a rather simple and straightforward task. Established standards can now be easily recalibrated[125] and measurement precision has reached an unprecedented level.[134] What is the next step? With the stability of the optical-frequency comb currently limited by the microwave reference used for phase locking f_{rep}, direct stabilization of comb components based on ultrastable optical references holds great promise. The initial demonstration of precision phase control of the comb shows that a single cw laser (along with its frequency-doubled companion output) can stabilize all comb lines (covering one octave of the optical frequency spectrum) to a level of 1–100 Hz at 1 s.[119] With control orthogonalization, we expect the system will be improved so that every comb line is phase locked to the cw reference below the 1 Hz level. Then we could generate a stable microwave frequency directly from a laser stabilized to an optical transition, essentially realizing an optical atomic clock. At the same time, an optical-frequency network spanning an entire optical octave (>300 THz) is established, with millions of regularly spaced frequency marks stable at the Hz level every 100 MHz, forming basically an optical-frequency synthesizer. The future looks very bright, considering the superior stability (10^{-15} at 1 s) offered by optical oscillators based on a single mercury ion,[126] a single ytterbiuim ion,[116] a single indium ion,[129] or cold calcium atoms.[126–128] Indeed, prototype optical clocks have recently been demonstrated based on single Hg^+ (Ref. 135) and I_2.[136] Within the next few years it will be amusing to witness friendly competition between the Cs and Rb fountain clocks and various optical clocks based on Hg^+, Ca, or some other suitable system.

ACKNOWLEDGMENTS

The authors wish to acknowledge the contributions of the many individuals who have contributed to this work. In particular they acknowledge S. A. Diddams and D. J. Jones for their substantial contributions in the lab, R. S. Windeler, J. K. Ranka, and A. J. Stentz (Bell Labs, Lucent Technologies) for providing the microstructure fiber, T. W. Hänsch and colleagues (Max-Planck Institute for Quantum Optics) for stimulating the work in this field and discussing their ongoing work with the authors. The authors thank L. Hollberg, J. Bergquist, T. Udem, L. S. Ma, T. H. Yoon, and T. Fortier for many useful discussions. This work at JILA was supported by NIST and NSF. The authors are staff members in the NIST Quantum Physics Division.

[1] G. E. Sterling and R. B. Monroe, *The Radio Manual* (Van Nostrand, New York, 1950).
[2] B. C. Young, F. C. Cruz, W. M. Itano, and J. C. Bergquist, Phys. Rev. Lett. **82**, 3799 (1999).
[3] R. J. Rafac, B. C. Young, J. A. Beall, W. M. Itano, D. J. Wineland, and J. C. Bergquist, Phys. Rev. Lett. **85**, 2462 (2000).
[4] N. F. Ramsey, J. Res. Natl. Bur. Stand. **88**, 301 (1983).
[5] C. Santarelli, P. Laurent, P. Lemonde, A. Clairon, A. G. Mann, S. Chang, A. N. Luiten, and C. Salomon, Phys. Rev. Lett. **82**, 4619 (1999).
[6] D. J. Berkeland, J. D. Miller, J. C. Bergquist, W. M. Itano, and D. J. Wineland, Phys. Rev. Lett. **80**, 2089 (1998).
[7] H. M. Goldenberg, D. Kleppner, and N. F. Ramsey, Phys. Rev. Lett. **8**, 361 (1960).
[8] C. Salomon, D. Hils, and J. L. Hall, J. Opt. Soc. Am. B **5**, 1576 (1988).
[9] R. W. P. Drever, J. L. Hall, F. V. Kowalski, J. Hough, G. M. Ford, A. J. Munley, and H. Ward, Appl. Phys. B: Photophys. Laser Chem. **B31**, 97 (1983).
[10] T. J. Quinn, Metrologia **36**, 211 (1999).
[11] M. Delabachelerie, K. Nakagawa, and M. Ohtsu, Opt. Lett. **19**, 840 (1994).
[12] J. Ye, L. S. Ma, and J. L. Hall, J. Opt. Soc. Am. B **15**, 6 (1998).
[13] J. Ye, L. S. Ma, and J. L. Hall, IEEE Trans. Instrum. Meas. **46**, 178 (1997).
[14] J. Ye, L. S. Ma, and J. L. Hall, J. Opt. Soc. Am. B **17**, 927 (2000).
[15] J. E. Bernard, A. A. Madej, L. Marmet, B. G. Whitford, K. J. Siemsen, and S. Cundy, Phys. Rev. Lett. **82**, 3228 (1999).
[16] M. Roberts, P. Taylor, G. P. Barwood, P. Gill, H. A. Klein, and W. R. C. Rowley, Phys. Rev. Lett. **78**, 1876 (1997).
[17] C. Tamm, D. Engelke, and V. Bühner, Phys. Rev. A **61**, 053405 (2000).
[18] E. Peik, J. Abel, T. Becker, J. von Zanthier, and H. Walther, Phys. Rev. A **60**, 439 (1999).
[19] J. L. Hall, M. Zhu, and P. Buch, J. Opt. Soc. Am. B **6**, 2194 (1989).
[20] F. Ruschewitz, J. L. Peng, H. Hinderthur, N. Schaffrath, K. Sengstock, and W. Ertmer, Phys. Rev. Lett. **80**, 3173 (1998).
[21] C. W. Oates, F. Bondu, R. W. Fox, and L. Hollberg, Eur. Phys. J. D **7**, 449 (1999).
[22] H. Katori, T. Ido, Y. Isoya, and M. Kuwata-Gonokami, Phys. Rev. Lett. **82**, 1116 (1999).
[23] K. R. Vogel, T. P. Dinneen, A. Gallagher, and J. L. Hall, IEEE Trans. Instrum. Meas. **48**, 618 (1999).
[24] J. R. Bochinski, T. Loftus, and T. W. Mossberg, Phys. Rev. A **61**, 041404 (2000).
[25] S. Guerandel, T. Badr, M. D. Plimmer, P. Juncar, and M. E. Himbert, Eur. Phys. J. D **10**, 33 (2000).
[26] J. Ye, L. Robertsson, S. Picard, L. S. Ma, and J. L. Hall, IEEE Trans. Instrum. Meas. **48**, 544 (1999).
[27] J. L. Hall, L. S. Ma, M. Taubman, B. Tiemann, F. L. Hong, O. Pfister, and J. Ye, IEEE Trans. Instrum. Meas. **48**, 583 (1999).
[28] J. L. Hall, J. Ye, L.-S. Ma, K. Vogel, and T. Dinneen, in *Laser Spectroscopy XIII*, edited by Z.-J. Wang, Z.-M. Zhang, and Y.-Z. Wang (World Scientific, Singapore, 1998), pp. 75–80.
[29] D. Hils and J. L. Hall, Phys. Rev. Lett. **64**, 1697 (1990).
[30] P. Fritschel, G. Gonzalez, B. Lantz, P. Saha, and M. Zucker, Phys. Rev. Lett. **80**, 3181 (1998).
[31] H. Mabuchi, J. Ye, and H. J. Kimble, Appl. Phys. B: Lasers Opt. **B68**, 1095 (1999).
[32] J. D. Prestage, R. L. Tjoelker, and L. Maleki, Phys. Rev. Lett. **74**, 3511 (1995).
[33] V. A. Dzuba, V. V. Flambaum, and J. K. Webb, Phys. Rev. A **59**, 230 (1999).
[34] V. A. Dzuba and V. V. Flambaum, Phys. Rev. A **61**, 034502 (2000).
[35] T. Udem, A. Huber, B. Gross, J. Reichert, M. Prevedelli, M. Weitz, and T. W. Hänsch, Phys. Rev. Lett. **79**, 2646 (1997).
[36] C. Schwob, L. Jozefowski, B. de Beauvoir, L. Hilico, F. Nez, L. Julien, F. Biraben, O. Acef, and A. Clairon, Phys. Rev. Lett. **82**, 4960 (1999).
[37] A. Peters, K. Y. Chung, B. Young, J. Hensley, and S. Chu, Philos. Trans. R. Soc. London, Ser. A **355**, 2223 (1997).
[38] T. Ikegami, S. Sudo, and Y. Sakai, *Frequency Stabilization of Semiconductor Laser Diodes* (Artech House, Norwood, MA, 1995).
[39] J. Ye and J. L. Hall, Opt. Lett. **24**, 1838 (1999).
[40] K. M. Evenson, J. S. Wells, F. R. Petersen, B. L. Danielson, and G. W. Day, Appl. Phys. Lett. **22**, 192 (1973).
[41] C. O. Weiss, G. Kramer, B. Lipphardt, and E. Garcia, IEEE J. Quantum Electron. **24**, 1970 (1988).
[42] A. Clairon, B. Dahmani, A. Filimon, and J. Rutman, IEEE Trans. Instrum. Meas. **34**, 265 (1985).
[43] C. R. Pollock, D. A. Jennings, F. R. Petersen, J. S. Wells, R. E. Drullinger, E. C. Beaty, and K. M. Evenson, Opt. Lett. **8**, 133 (1983).
[44] D. A. Jennings, C. R. Pollock, F. R. Petersen, R. E. Drullinger, K. M. Evenson, J. S. Wells, J. L. Hall, and H. P. Layer, Opt. Lett. **8**, 136 (1983).
[45] O. Acef, J. J. Zondy, M. Abed, D. G. Rovera, A. H. Gerard, A. Clairon, P. Laurent, Y. Millerioux, and P. Juncar, Opt. Commun. **97**, 29 (1993).
[46] R. L. Barger and J. L. Hall, Appl. Phys. Lett. **22**, 196 (1973).
[47] H. Schnatz, B. Lipphardt, J. Helmcke, F. Riehle, and G. Zinner, Phys. Rev. Lett. **76**, 18 (1996).

[48] H. R. Telle, D. Meschede, and T. W. Hänsch, Opt. Lett. **15**, 532 (1990).
[49] N. C. Wong, Opt. Lett. **15**, 1129 (1990).
[50] M. Kourogi, K. Nakagawa, and M. Ohtsu, IEEE J. Quantum Electron. **29**, 2693 (1993).
[51] L. R. Brothers, D. Lee, and N. C. Wong, Opt. Lett. **19**, 245 (1994).
[52] D. A. van Baak and L. Hollberg, Opt. Lett. **19**, 1586 (1994).
[53] O. Pfister, M. Murtz, J. S. Wells, L. Hollberg, and J. T. Murray, Opt. Lett. **21**, 1387 (1996).
[54] P. T. Nee and N. C. Wong, Opt. Lett. **23**, 46 (1998).
[55] C. Koch and H. R. Telle, J. Opt. Soc. Am. B **13**, 1666 (1996).
[56] J. N. Eckstein, A. I. Ferguson, and T. W. Hänsch, Phys. Rev. Lett. **40**, 847 (1978).
[57] J. L. Hall, M. Taubman, S. A. Diddams, B. Tiemann, J. Ye, L. S. Ma, D. J. Jones, and S. T. Cundiff, in *Laser Spectroscopy XIII*, edited by R. Blatt, J. Eschner, D. Leibfried, and F. Schmidt-Kaler (World Scientific, Singapore, 1999), pp. 51–60.
[58] B. G. Whitford, Appl. Phys. B: Photophys. Laser Chem. **B35**, 119 (1984).
[59] F. Nez *et al.*, Phys. Rev. Lett. **69**, 2326 (1992).
[60] S. Slyusarev, T. Ikegami, and S. Ohshima, Opt. Lett. **24**, 1856 (1999).
[61] A. Douillet, J. J. Zondy, A. Yelisseyev, S. Lobanov, and L. Isaenko, IEEE Trans. Ultrason. Ferroelectr. Freq. Control **47**, 1127 (2000).
[62] K. Imai, Y. Zhao, M. Kourogi, B. Widiyatmoko, and M. Ohtsu, Opt. Lett. **24**, 214 (1999).
[63] K. Imai, M. Kourogi, and M. Ohtsu, IEEE J. Quantum Electron. **34**, 54 (1998).
[64] J. Ye, L. S. Ma, T. Day, and J. L. Hall, Opt. Lett. **22**, 301 (1997).
[65] S. A. Diddams, L. S. Ma, J. Ye, and J. L. Hall, Opt. Lett. **24**, 1747 (1999).
[66] K. Nakagawa, M. de Labachelerie, Y. Awaji, and M. Kourogi, J. Opt. Soc. Am. B **13**, 2708 (1996).
[67] Th. Udem, J. Reichert, T. W. Hänsch, and M. Kourogi, Phys. Rev. A **62**, 031801 (2000).
[68] P. Dubé (personal communication 1997).
[69] J. Ye, Ph.D. thesis, University of Colorado, Boulder, CO, 1997.
[70] T. Kobayashi, T. Sueta, Y. Cho, and Y. Matsuo, Appl. Phys. Lett. **21**, 341 (1972).
[71] G. M. Macfarlane, A. S. Bell, E. Riis, and A. I. Ferguson, Opt. Lett. **21**, 534 (1996).
[72] K. P. Ho and J. M. Kahn, IEEE Photonics Technol. Lett. **5**, 721 (1993).
[73] L. R. Brothers and N. C. Wong, Opt. Lett. **22**, 1015 (1997).
[74] T. W. Hänsch, in *Tunable Lasers and Applications*, edited by A. Mooradain, T. Jaeger, and P. Stokseth (Springer, Berlin, 1976).
[75] E. V. Baklanov and V. P. Chebotaev, Sov. J. Quantum Electron. **7**, 1252 (1977).
[76] R. Teets, J. Eckstein, and T. W. Hänsch, Phys. Rev. Lett. **38**, 760 (1977).
[77] M. M. Salour, Rev. Mod. Phys. **50**, 667 (1978).
[78] A. I. Ferguson and R. A. Taylor, Proc. SPIE **369**, 366 (1983).
[79] S. R. Bramwell, D. M. Kane, and A. I. Ferguson, Opt. Commun. **56**, 112 (1985).
[80] S. R. Bramwell, D. M. Kane, and A. I. Ferguson, J. Opt. Soc. Am. B **3**, 208 (1986).
[81] D. M. Kane, S. R. Bramwell and A. I. Ferguson, Appl. Phys. B: Photophys. Laser Chem. **39**, 171 (1986).
[82] D. J. Wineland, J. C. Bergquist, W. M. Itano, F. Diedrich, and C. S. Weimer, in *The Hydrogen Atom*, edited by G. F. Bassani, M. Inguscio and T. W. Hänsch (Springer, Berlin, 1989), pp. 123–133.
[83] H. R. Telle, G. Steinmeyer, A. E. Dunlop, J. Stenger, D. H. Sutter, and U. Keller, Appl. Phys. B: Lasers Opt. **B69**, 327 (1999).
[84] T. Udem, J. Reichert, R. Holzwarth, and T. W. Hänsch, Opt. Lett. **24**, 881 (1999).
[85] T. Udem, J. Reichert, R. Holzwarth, and T. W. Hänsch, Phys. Rev. Lett. **82**, 3568 (1999).
[86] J. Reichert, R. Holzwarth, T. Udem, and T. W. Hänsch, Opt. Commun. **172**, 59 (1999).
[87] J. von Zanthier *et al.*, Opt. Commun. **166**, 57 (1999).
[88] S. A. Diddams, D. J. Jones, L. S. Ma, S. T. Cundiff, and J. L. Hall, Opt. Lett. **25**, 186 (2000).
[89] D. J. Jones, S. A. Diddams, J. K. Ranka, A. Stentz, R. S. Windeler, J. L. Hall, and S. T. Cundiff, Science **288**, 635 (2000).
[90] D. J. Jones, S. A. Diddams, M. S. Taubman, S. T. Cundiff, L. S. Ma, and J. L. Hall, Opt. Lett. **25**, 308 (2000).
[91] S. A. Diddams *et al.*, Phys. Rev. Lett. **84**, 5102 (2000).
[92] J. Reichert, M. Niering, R. Holzwarth, M. Weitz, T. Udem, and T. W. Hänsch, Phys. Rev. Lett. **84**, 3232 (2000).
[93] T. H. Yoon, A. Marian, J. L. Hall, and J. Ye, Phys. Rev. A **63**, 011402 (2000).
[94] D. K. Negus, L. Spinelli, N. Goldblatt, and G. Feugnet, in *Advanced Solid-State Lasers* (OSA, Washington, DC, 1991), Vol. 10.
[95] D. E. Spence, P. N. Kean, and W. Sibbett, Opt. Lett. **16**, 42 (1991).
[96] M. T. Asaki, C. P. Huang, D. Garvey, J. P. Zhou, H. C. Kapteyn, and M. M. Murnane, Opt. Lett. **18**, 977 (1993).
[97] J. K. Ranka, R. S. Windeler, and A. J. Stentz, Opt. Lett. **25**, 25 (2000).
[98] J.-C. Diels and W. Rudolph, *Ultrashort Laser Pulse Phenomena: Fundamentals, Techniques, and Applications on a Femtosecond Time Scale* (Academic, San Diego, 1996).
[99] E. P. Ippen, Appl. Phys. B: Lasers Opt. **B58**, 159 (1994).
[100] R. L. Fork, O. E. Martinez, and J. P. Gordon, Opt. Lett. **9**, 150 (1984).
[101] U. Morgner *et al.*, Opt. Lett. **24**, 411 (1999).
[102] D. H. Sutter, G. Steinmeyer, L. Gallmann, N. Matuschek, F. Morier-Genoud, U. Keller, V. Scheuer, G. Angelow, and T. Tschudi, Opt. Lett. **24**, 631 (1999).
[103] R. L. Fork, C. H. B. Cruz, P. C. Becker, and C. V. Shank, Opt. Lett. **12**, 483 (1987).
[104] I. P. Christov, M. M. Murnane, H. C. Kapteyn, J. P. Zhou, and C. P. Huang, Opt. Lett. **19**, 1465 (1994).
[105] R. Szipocs, K. Ferencz, C. Spielmann, and F. Krausz, Opt. Lett. **19**, 201 (1994).
[106] S. T. Cundiff and S. A. Diddams (unpublished).
[107] R. J. Jones, J. C. Diels, J. Jasapara, and W. Rudolph, Opt. Commun. **175**, 409 (2000).
[108] S. B. Darack, D. R. Dykaar, and G. T. Harvey, Opt. Lett. **16**, 1677 (1991).
[109] A. Apolonski, A. Poppe, G. Tempea, C. Spielmann, T. Udem, R. Holzwarth, T. W. Hänsch, and F. Krausz, Phys. Rev. Lett. **85**, 740 (2000).
[110] J. K. Ranka, R. S. Windeler, and A. J. Stentz, Opt. Lett. **25**, 796 (2000).
[111] L. Xu, M. W. Kimmel, P. O'Shea, R. Trebino, J. K. Ranka, R. S. Windeler, and A. J. Stentz, in *XII International Conference on Ultrafast Phenomena*, edited by S. M. T. Elsaesser, M. M. Murnane, and N. F. Scherer (Springer, Charleston, SC, 2000), pp. 129–131.
[112] S. A. Diddams (personal communication 2000).
[113] R. M. Shelby, M. D. Levenson, and P. W. Bayer, Phys. Rev. B **31**, 5244 (1985).
[114] A. J. Poustie, Opt. Lett. **17**, 574 (1992).
[115] A. J. Poustie, J. Opt. Soc. Am. B **10**, 691 (1993).
[116] J. Stenger, C. Tamm, N. Haverkamp, S. Weyers, and H. R. Telle, Opt. Lett. (in press).
[117] H. R. Telle, B. Lipphardt, and J. Stenger, Appl. Phys. B: Lasers Opt. (submitted).
[118] K. F. Kwong, D. Yankelevich, K. C. Chu, J. P. Heritage, and A. Dienes, Opt. Lett. **18**, 558 (1993).
[119] J. Ye, J. L. Hall, and S. A. Diddams, Opt. Lett. **25**, 1675 (2000).
[120] L. Xu, C. Spielmann, A. Poppe, T. Brabec, F. Krausz, and T. W. Hänsch, Opt. Lett. **21**, 2008 (1996).
[121] R. Holzwarth, T. Udem, T. W. Hänsch, J. C. Knight, W. J. Wadsworth, and P. S. J. Russell, Phys. Rev. Lett. **85**, 2264 (2000).
[122] H. A. Haus and E. P. Ippen (unpublished).
[123] J. Stenger and H. R. Telle, Opt. Lett. **25**, 1553 (2000).
[124] R. Ell *et al.*, Opt. Lett. **26**, 373 (2001).
[125] J. Ye, T. H. Yoon, J. L. Hall, A. A. Madej, J. E. Bernard, K. J. Siemsen, L. Marmet, J.-M. Chartier, and A. Chariter, Phys. Rev. Lett. **85**, 3797 (2000).
[126] T. Udem *et al.*, Phys. Rev. Lett. **86**, 4996 (2001).
[127] K. R. Vogel *et al.*, Opt. Lett. **26**, 102 (2001).
[128] J. Stenger, T. Binnewies, G. Wilpers, F. Riehle, H. R. Telle, J. K. Ranka, R. S. Windeler, and A. J. Stentz, Phys. Rev. A **63**, 021802 (2001).
[129] J. von Zanthier *et al.*, Opt. Lett. **25**, 1729 (2000).
[130] C. G. Durfee, A. R. Rundquist, S. Backus, C. Herne, M. M. Murnane, and H. C. Kapteyn, Phys. Rev. Lett. **83**, 2187 (1999).
[131] A. Bartels, T. Dekorsy, and H. Kurz, Opt. Lett. **24**, 996 (1999).
[132] F. X. Kärtner, U. Morgner, T. Schibli, J. G. Fujimoto, E. P. Ippen, V. Scheuer, G. Angelow, and T. Tschudi, J. Opt. Soc. Am. B **18**, 882 (2001).
[133] E. Cormier and P. Lambropoulos, Eur. Phys. J. D **2**, 15 (1998).
[134] M. Niering *et al.*, Phys. Rev. Lett. **84**, 5496 (2000).
[135] S. A. Diddams *et al.*, Science **293**, 825 (2001).
[136] J. Ye, L. S. Ma, and J. L. Hall, Phys. Rev. Lett. (submitted).